Critical Reviews in Biochemistry and Molecular Biology, 39:165–195, 2004

ISSN: 1040-9238 print / 1549-7798 online
DOI: 10.1080/10409230490496577

Life with Carbon Monoxide

Stephen W. Ragsdale

Department of Biochemistry, Beadle Center, University of Nebraska, Lincoln, NE, USA

This review focuses on how microbes live on CO as a sole source of carbon and energy and with CO by generating carbon monoxide as a metabolic intermediate. The use of CO is a property of organisms that use the Wood-L jungdahl pathway of autotrophic growth. The review discusses when CO metabolism originated, when and how it was discovered, and what properties of CO are ideal for microbial growth. How CO sensing by a heme-containing transcriptional regulatory protein activates the expression of CO metabolism-linked genes is described. Two metalloenzymes are the cornerstones of growth with CO: CO dehydrogenase (CODH) and acetyl-CoA synthase (ACS). CODH oxidizes CO to CO_2, providing low-potential electrons for the cell, or alternatively reduces CO_2 to CO. The latter reaction, when coupled to ACS, forms a machine for generating acetyl-CoA from CO_2 for cell carbon synthesis. The recently solved crystal structures of CODH and ACS along with spectroscopic measurements and computational studies provide insights into novel bio-organometallic catalytic mechanisms and into the nature of a 140 Å gas channel that coordinates the generation and utilization of CO. The enzymes that are coupled to CODH/ACS are also described, with a focus on a corrinoid protein, a methyltransferase, and pyruvate ferredoxin oxidoreductase.

Keywords acetogenesis, methanogenesis, carbon dioxide fixation, nickel, iron-sulfur, metallobiochemistry, CO dehydrogenase, acetyl-CoA synthase, CO_2 fixation, molybdopterin, iron-sulfur cluster, evolution, heme, gene regulation, nickel, metalloenzyme, copper, substrate channeling, EPR spectroscopy, IR spectroscopy, corrinoid protein, vitamin B_{12}, Wood-Ljungdahl pathway, autotrophic growth, methyltransferase, pyruvate ferredoxin oxidoreductase, pyruvate synthase, CH_3-H_4folate, anaerobe

PROSPECTIVE AND INTRODUCTION

This review will focus on how microbes live, not only on CO as a sole source of carbon and energy, but also with CO by generating carbon monoxide as a metabolic intermediate. Since CO is an inorganic carbon source, we will consider growth on CO as autotrophic, although Wilhelm Pfeffer's 1897 definition, which is still used today, includes organisms able to synthesize their cell substance from inorganic carbonate as their main source of carbon (Brock & Schlegel, 1989). The use of CO, a toxic gas to animals, as a metabolic building block is an interesting property of certain classes of diverse organisms that can grow on CO_2 by any of the known CO_2 fixation pathways as long as they have a mechanism for converting CO into CO_2. This review will focus on the enzyme, CO dehydrogenase (CODH), that interconverts CO and CO_2. It will also focus on a CO_2 and CO fixation mechanism called the *Wood-Ljungdahl pathway* (Figure 1). This figure shows growth on glucose; however, as described below, this pathway allows for autotrophic growth on CO_2 with electrons coming from H_2 oxidation, on CO serving as both a carbon and energy source, and on other compounds. Several questions related to the microbial metabolism of CO will be discussed. When did microbial CO metabolism originate and how was it discovered? Is there reasonable evidence for the hypothesis that the first living organisms metabolized CO? What properties of CO make it ideal for growth of certain microbes?

It is timely to describe recent exciting findings related to the two metalloenzymes at the foundation of CO metabolism: (CODH) and acetyl-CoA synthase (ACS). CODH is a redox-chemical transformer that generates high-energy electrons as it catalyzes the oxidation of CO to CO_2 (Equation (1)). The CO_2 is then fixed into cellular carbon by one of the reductive CO_2 fixation pathways, like the Calvin-Benson-Bassham Cycle, the reverse tricarboxylic acid (TCA) cycle, the 3-hydroxypropionate cycle, or the Wood-Ljungdahl pathway. In at least some of these organisms (Youn *et al.*, 2004), *e.g.*, *Rhodospirillum rubrum*, CO is sensed by binding to a heme-containing transcriptional regulatory protein (Aono *et al.*, 1996; Shelver *et al.*, 1997) that activates the expression of a battery of structural, metal incorporation, and maturation genes (Fox *et al.*, 1996).

Editor: James A. Imlay
Address correspondence to Stephen W. Ragsdale, Department of Biochemistry, Beadle Center, 19th and Vine Streets, University of Nebraska, Lincoln, NE, 68588-0664, USA. E-mail: sragsdale1@unl.edu

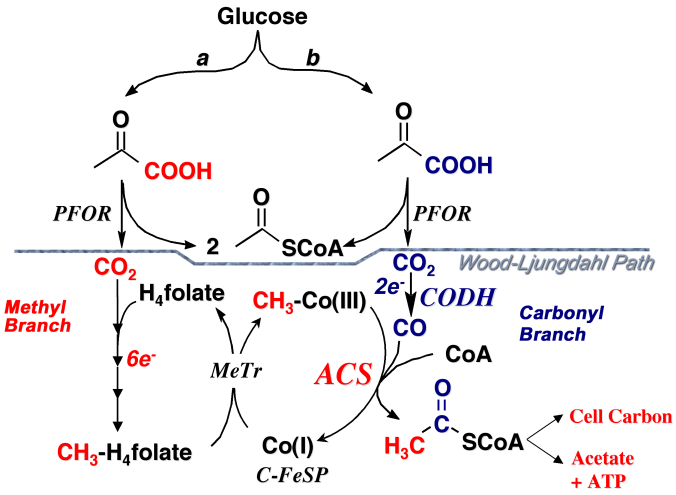

FIG. 1. The Wood-Ljungdahl pathway of autotrophic CO and CO_2 fixation. CODH, CO dehydrogenase; ACS, acetyl-CoA synthase; MeTr, methyltransferase; CFeSP, Corrinoid iron-sulfur protein. PFOR, pyruvate ferredoxin oxidoreductase. Reactions leading to the formation of the methyl group of acetyl-CoA are colored red, while those leading to the carbonyl group are colored blue.

When the redox-chemical transformer CODH is coupled to ACS, it forms a powerful machine for generating the ubiquitous building block acetyl-CoA from CO_2, a methyl group, and CoA (Figure 2). In this case, CODH reduces CO_2 to CO, which is the source of the carbonyl group of acetyl-CoA in the final steps of the Wood-Ljungdahl pathway. ACS is a NiFeS enzyme that condenses Coenzyme A, a methyl group, and CO generated by CODH to form acetyl-CoA (Equation (2)). The methyl group is donated by an organometallic methylcobamide (a vitamin B_{12} derivative) species on a protein called the *corrinoid iron-sulfur protein* (CFeSP). The structure and function of the CFeSP, and how this methyl-Co intermediate is generated in a methyltransferase-catalyzed reaction, are discussed more briefly since these aspects of the Wood-Ljungdahl pathway have been recently reviewed (Banerjee & Ragsdale, 2003).

This review describes the recently solved crystal structures of CODH and ACS, which have prompted a reinterpretation of spectroscopic studies performed over the past two decades. These structures, spectroscopic measurements, and computational studies provide insights into the novel bioorganometallic catalytic mechanisms that underlie the Wood-Ljungdahl pathway and resemble some important industrial reactions. Generation and utilization of the toxic gas CO occur at active sites that are 70 Å apart. How are the activities of these two sites coordinated so that CO does not escape from the enzyme? The nature of a channel and the evidence for kinetic coupling between the two active sites is described. This gas channel is compared to other gas channels that have been described in nature.

Life with CO involves the conceptually simplistic stepwise condensation of two one-carbon compounds to form a two-carbon acetyl unit followed by the successive addition of one-carbon units. Recent studies on pyruvate ferredoxin oxidoreductase (PFOR), the enzyme that generates pyruvate (Equation (3)), the first three-carbon unit, are only briefly described since it has been recently reviewed (Ragsdale, 2003b). PFOR is extremely important because it also is a source of CO_2 and low-potential electrons when the cells grow on sugars. Further reactions that interface the Wood-Ljungdahl pathway to the synthesis of cellular components are described. The review also summarizes some studies of how CO metabolism is regulated and the radical differences in regulatory systems between those organisms that function to oxidize CO and those that

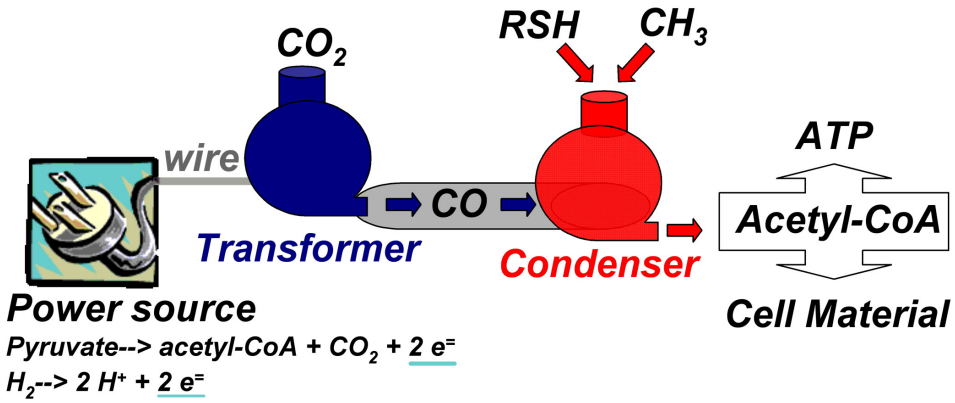

FIG. 2. CODH/ACS, a nanomachine. CODH is represented as a transformer for generating CO and ACS as a condenser that converts CO, a methyl group, and CoA to form acetyl-CoA, a cellular biosynthetic building block and source of ATP.

generate and utilize it.

$$2 \text{ electrons} + 2\,H^+ + CO_2 \leftrightarrow CO + H_2O \quad [1]$$

$$CO + CH_3{-}CFeSP + CoA \rightarrow \text{acetyl-CoA} + CFeSP + H^+ \quad [2]$$

$$\text{Pyruvate} + CoA \leftrightarrow \text{acetyl-CoA} + CO_2 + H^+ + 2 \text{ electrons} \quad [3]$$

Discovery of Microbial CO Metabolism

Enzymatic CO oxidation was discovered around 1903, when thin films of bacteria were found growing in a purely mineral medium with coal gas, a mixture of H_2 and CO, as the carbon source (Beijerinck & van Delden, 1903). Kaserer recognized that a similar bacterial culture was growing on a carbon-containing component of the atmosphere (Kaserer, 1906) but two decades passed before the first bacterial strain that could grow on CO was isolated (Lantzsch, 1922). It is now known that CO can serve as a carbon and electron source for many bacteria, including anaerobes such as *Moorella thermoacetica* (Daniel *et al.*, 1990; Kerby & Zeikus, 1983), some purple sulfur bacteria akin to *R. rubrum* (Uffen, 1983), and *Carboxydothermus hydrogenoformans* (Svetlichny *et al.*, 1991), as well as some aerobic carboxydobacteria like *Oligotropha carboxidovorans* (Meyer & Schlegel, 1983). These are the organisms in which CO metabolism has been most thoroughly studied.

This area of CO oxidation and synthesis may eventually have a practical benefit. Development of catalysts that can be used on a large scale to lower CO concentrations in heavily polluted areas is one significant challenge to science. Furthermore, many scientists and government policy makers would be interested in ways to decrease the concentration of CO_2, a potent greenhouse gas that is relatively inert. One possibility is to develop biomimetic catalysts since CODH rapidly and efficiently oxidizes CO at rates between 4,000 and 40,000 s^{-1}, depending on the source, and reduces CO_2 ($\sim$11 s^{-1}) (Kumar *et al.*, 1994; Lindahl *et al.*, 1990a) with virtually no overpotential and under mild conditions.

Why CO? Importance of CO Metabolism

CO Uptake and Oxidation. CO is a toxic, odorless, and tasteless gas that is produced by natural and anthropogenic processes by the incomplete combustion of organic materials. The OSHA limit for CO is 50 ppm continuous exposure for 8 h, because mild effects of CO poisoning are observed within 2–3 h when CO levels climb to 200 ppm and exposure to 1000 ppm for 1 h is fatal. CO is produced by incomplete combustion of fuel, for example, from motor vehicle exhaust, which contributes about 60% of all CO emissions in the USA. The major natural CO sources are methane and natural hydrocarbon oxidation. CO emissions, which are nearly equally distributed between natural and manmade sources, lead to atmospheric levels of CO ranging from about 0.1 ppm in rural areas to approximately 30 ppm in urban areas. Nevertheless, some microbes base their autotrophic metabolism on such trace levels by oxidizing CO at rates as high as 40,000 mol CO per mol enzyme per second and catalytic efficiencies reaching 2×10^9 $M^{-1}s^{-1}$ (Svetlitchnyi *et al.*, 2001). Microbial CO metabolism is quite important to all animals, since about 10^8 tons of CO are removed from the lower atmosphere of the earth by bacterial oxidation every year (Bartholomew & Alexander, 1979), which helps to maintain ambient CO below toxic levels.

CO can serve as both a carbon and electron source for organisms that use the Wood-Ljungdahl pathway. First, it can provide extremely low potential electrons for reducing cellular electron carriers. With a CO_2/CO reduction potential of -558 mV (pH 7.0; Grahame & Demoll, 1995), CO is about 1000-fold more potent than NADH.

Second, CO has ideal chemical properties for the bioorganometallic reaction sequence in the Wood-Ljungdahl pathway. Containing a multiple bond, C≡O is a weak Lewis base and an unsaturated soft ligand that can accept metal dπ electrons by a process called *back bonding*. Thus, CO acts both as a sigma donor and pi acceptor that can form stable complexes with the low valent states of the metal sites in enzymes. Of course, this property also makes CO a strong inhibitor of metalloproteins that use low valent metals in their functions, like hydrogenases and hemeproteins that function to bind O_2 or other diatomic gases. Besides its ability to serve as a strong ligand for transition metals, the metal carbonyls that are produced are known to undergo facile ligand substitutions, insertions, eliminations, and nucleophilic additions (Crabtree, 1988; Lukehart, 1985). These reactions can be fine tuned by altering the polarization of the metal-bound CO. For example, nucleophilic addition reactions (*e.g.*, attack by hydroxide anion during CO oxidation) and migratory insertion reactions (*e.g.*, methyl addition during acetyl-CoA synthesis) are promoted by increasing the electrophilicity of the CO carbon. On the other hand, an electrophilic attack at oxygen would be favored by increasing the nucleophilicity at the CO oxygen. It will be exciting for computational chemists to consider ways that the Ni active sites of CODH and ACS, which both appear to form Ni-CO complexes (Chen *et al.*, 2003), have been crafted to enhance the particular required reaction and prevent other potentially inhibitory reactions. For example, the M-CO complex plays a key role in industrial organometallic catalysis

reactions, including catalytic carbonylation, the Fischer-Tropsch reaction, reactions with syn Gas, hydroformylation reactions, homologation reactions, the Water-Gas Shift Reaction, and hydrogenation reactions using water as the hydrogen source (Ford & Rokicki, 1988). Some important strides in computational studies of the CODH and ACS reactions have already been made (Schenker & Brunold, 2003; Webster *et al.*, 2004).

Another reason that CO is an excellent metabolite for organisms that use the Wood-Ljungdahl pathway is that it is already dehydrated and at the oxidation state of the carbonyl group of acetyl-CoA, which is a key building block for cellular anabolism and an important source of ATP.

CO Production. Organisms that use the Wood-Ljungdahl pathway generate CO from CO_2 or pyruvate as a metabolic intermediate (Menon & Ragsdale, 1996a). Humans also produce CO as a signal molecule (Verma *et al.*, 1993) during heme metabolism by heme oxygenase (Boehning & Snyder, 2003). CO is also biologically generated during conversion of S-methylthioadenosine to methionine (Dai *et al.*, 1999), aromatic amino acid metabolism by bacteria (Hino & Tauchi, 1987), aldehyde decarbonylation by plants (Cheesbrough & Kolattukudy, 1984), and heme degradation by heme oxygenase (Tenhunen *et al.*, 1969). The latter reaction appears to allow CO to serve as a neurotransmitter (Verma *et al.*, 1993) and to regulate vascular cGMP levels (Morita *et al.*, 1995). Of the above reactions, it appears that only the Wood-Ljungdahl pathway is capable of direct metabolism of CO.

A major focus of this review is on anaerobic microbes that catalyze the reduction of CO_2 to CO with CODH. As shown in Figure 1, CO_2 can come from the decarboxylation of pyruvate, which is generated from sugars by the Embden-Meyerhof pathway. It also can be formed from the carboxyl group of benzoic acid and its derivatives (Hsu *et al.*, 1990a, 1990b). Some anaerobic microbes, like acetogens and methanogens, can use the Wood-Ljungdahl pathway to utilize CO_2 from the growth medium. The coupling of pyruvate oxidation to CO synthesis and to acetyl-CoA formation has been well studied in *M. thermoacetica* (Menon & Ragsdale, 1996a, 1996b, 1997). PFOR catalyzes the conversion of pyruvate to acetyl-CoA and CO_2 (Equation (3)). Then CODH reduces CO_2 to CO (Equation (1)). Finally, ACS, which is the other subunit of the bifunctional CODH/ACS, catalyzes the condensation of CO with a methyl group and coenzyme A to form acetyl-CoA (Equation (2)). Acetyl-CoA is then used in ATP generation or in cellular biosynthesis (Figure 1). Thus, the bifunctional enzyme CODH/ACS plays an essential role in energy metabolism and cellular biosynthesis.

Since these organisms generate CO during their growth, why aren't they environmentally hazardous? On the contrary, we harbor acetogens and methanogens in our gastrointestinal tract (Dore *et al.*, 1995; Wolin & Miller, 1994). Surprisingly, although cultures of *M. thermoacetica* growing on glucose with a 100% CO_2 gas phase have a vast potential for CO production, they only produce about 50 ppb CO (Diekert *et al.*, 1984). As discussed below, there is tight regulation of CO production and CO utilization. There is strong evidence that the CO produced during acetyl-CoA biosynthesis is sequestered in a molecular channel, which maintains the CO concentration below toxic levels for the host organisms and allows organisms to retain this valuable carbon and energy source without having it escape into the environment.

CO and CO_2 Fixation with an Evolutionary Perspective

Since CO and CO_2 are in equilibrium, CO metabolism is linked to the global carbon cycle, which involves the oxidation of organic carbon to CO_2 by heterotrophic organisms as an energy source and the replenishment of fixed organic carbon by autotrophic organisms in a reductive process called CO_2 fixation. CO_2 is returned to the carbon cycle by one of the following pathways: the Calvin-Benson-Basham cycle, the reductive TCA cycle, the Wood-Ljungdahl (acetyl-CoA) pathway (Equation (4)), or the 3-hydroxypropionate (Menendez *et al.*, 1999) cycle. The Calvin-Benson-Basham cycle requires energy, which is driven by photosynthesis or chemoautotrophy. On the other hand, the Wood-Ljungdahl pathway, in coupling H_2 oxidation to CO_2 reduction, is exergonic and conserves energy for the organism by electron transfer-linked phosphorylation (Hugenholtz & Ljungdahl, 1989).

Perhaps the use of CO remains from the early atmospheric conditions when life first evolved around 4 billion years ago. This follows from the hypothesis that the first organisms were autotrophic (Huber & Wachtershauser, 1997; Russell *et al.*, 1998; Russell & Hall, 1997). Based on the patterns of isotopic fractionation between ^{12}C and ^{13}C, the sedimentary carbon record indicates that autotrophic growth developed soon after the earth became habitable (Schidlowski *et al.*, 1983). Furthermore, anaerobic organisms using the Wood-Ljungdahl pathway have an isotope fractionation pattern consistent with the hypothesis that they may have been using inorganic compounds like CO and H_2 as an energy source and CO_2 as an electron accepter approximately 1 billion years before O_2 appeared (Brock, 1989). Since volcanic gases can contain as high as 1% CO, perhaps early life forms evolving in volcanic sites or hydrothermal vents could have used CO as their carbon and energy source. If this scenario is correct, CO

metabolism today can be viewed as the extant survivor of early metabolic processes (Huber & Wachtershauser, 1997).

$$4\,H_2 + 2\,CO_2 \rightarrow CH_3COO^- + H^+ + 2\,H_2O$$
$$\Delta G^{0\prime} = -95\ \text{kJ/mol} \qquad [4]$$

MICROBES THAT CAN METABOLIZE CARBON MONOXIDE

Aerobic CO Metabolism

Carboxydotrophic bacteria are aerobic microbes that grow on CO as their sole source of carbon and energy. These microbes transfer the electrons derived from CODH-catalyzed CO oxidation through an electron transport chain that finally reduces oxygen according to Equation (5) (Meyer & Rhode, 1984). The CO_2 is assimilated into cell carbon through the Calvin-Benson-Basham pathway. The carboxydobacteria are well suited for a role in CO detoxification in the environment because they have a high propensity for uptake of this trace gas, with Km values as low as 0.6 μM (Meyer *et al.*, 1993); however, their turnover numbers are nearly 1000-fold lower than those of the anaerobic Ni-CODHs (Gnida *et al.*, 2003). These enzymes are called Mo-CODHs because they contain molybdopterin (Mo-CODH) and share many properties with the Mo hydroxylases, such as sulfite oxidase and xanthine oxidase.

$$O_2 + 2.19\ CO \rightarrow 1.83\ CO_2 + 0.36\ \text{Cell Carbon} \qquad [5]$$

Genes and Regulation of Anaerobic CO Metabolism

CO Sensing and Oxidation by the coo *System. R. rubrum*, which utilizes CO as a source of carbon and energy, contains the *coo* regulon, consisting of at least two operons (Figure 3). When microbes sense the presence of CO, expression of the coo genes is induced at least 1000-fold (Shelver *et al.*, 1995). The first operon in the *coo* gene cluster encodes a hydrogenase and the proteins involved in generating the active form of the enzyme, while the second operon consists of the genes for CODH (*cooS*), a membrane-associated electron transfer FeS protein (*cooF*), and at least three other genes involved in generating the NiFeS-active site of CooS. CooC is a Ni insertase (Jeon *et al.*, 2001) that is similar to ureE in binding and hydrolyzing ATP or GTP (Song *et al.*, 2001). CooJ also is similar to UreE and contains a His-rich C-terminus that can bind as many as four Ni ions (Watt & Ludden, 1998). The role of CooT is less well understood, but it appears to aid in ensuring that Ni, instead of other metals, are incorporated into the active site of CO oxidation, called Cluster C (below) (Kerby *et al.*, 1997). The proteins involved in Ni incorporation into CODH and their functions have been reviewed (Watt & Ludden, 1999).

CO is sensed by a heme that is bound to CooA, which is a member of a large family of transcriptional activators that include the cAMP regulatory protein (CRP) and fumarate nitrate reductase regulator (FNR) (Aono, 2003). These proteins contain an N-terminal effector binding domain, which in CooA is a heme wrapped in a beta roll structure, and a C-terminal helix-turn-helix DNA binding domain (Figure 4) (Lanzilotta *et al.*, 2000). In the unactivated ferrous form of CooA, a histidine residue (His77)

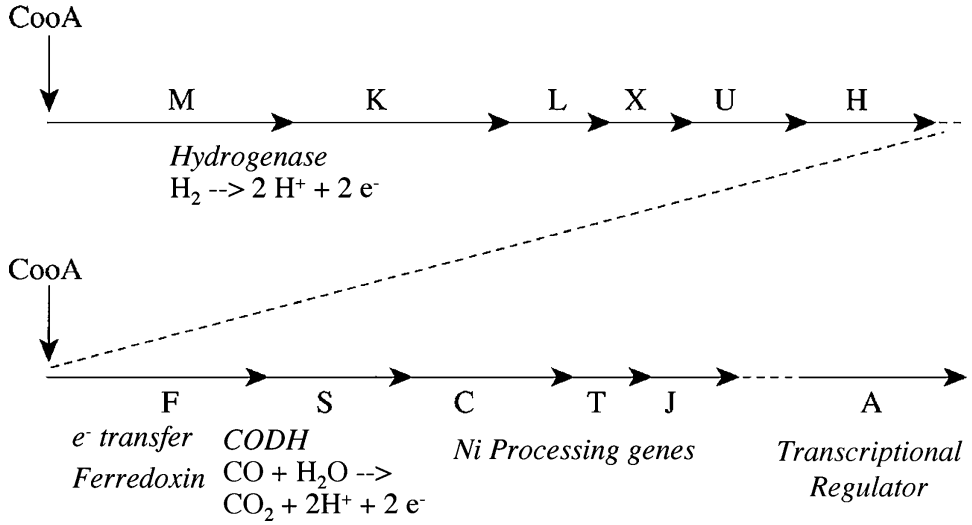

FIG. 3. Coo Regulon. In the presence of CO, CooA binds to the promotor regions to activate transcription of two operons. One operon encodes a membrane-bound hydrogenase and its accessory genes, while the other encodes CODH and its accessory proteins. Modified from Watt and Ludden (1999).

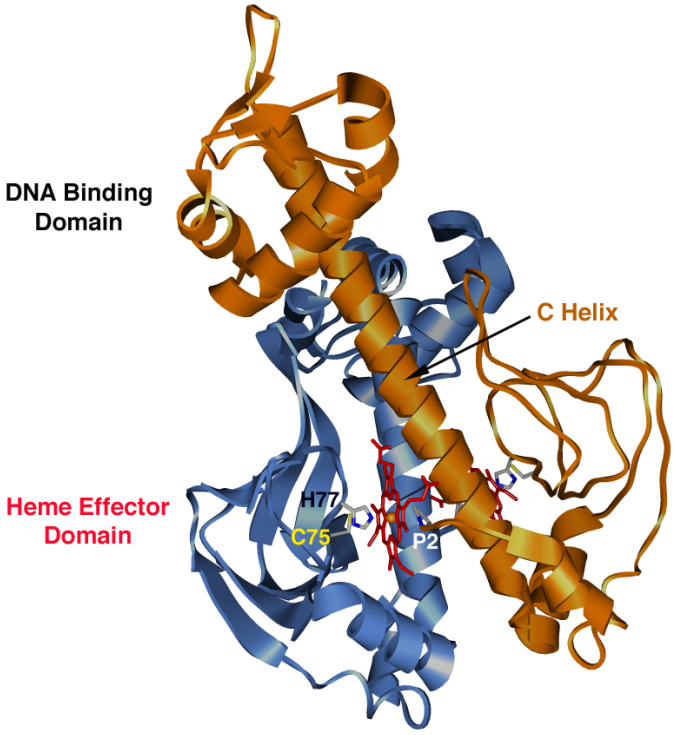

FIG. 4. The structure of CooA. The two monomers are colored orange or blue and the heme is shown in red. Generated using Chimera from PDB accession number 1FT9.

and, surprisingly, the amino terminal proline (Pro2) serve as the heme ligands (Lanzilotta *et al.*, 2000). Although only the structure of reduced CooA is known, spectroscopic studies have uncovered a complex series of ligand switches. While the ferrous heme of CooA is 6-coordinate with Pro2 and His77 as the axial ligands, Cys75 and Pro2 are the ligands in the ferric state (Aono, 2003; Coyle *et al.*, 2003; Yamamoto *et al.*, 2001). CO binds to the ferrous state (with Pro and His ligands), replacing the proline ligand, which causes a major structural rearrangement, promoting the formation of a productive complex with RNA poymerase and the *coo* promoter region (Aono, 2003). By mutagenesis, the sites of interaction between CooA and RNA polymerase have been mapped (Leduc *et al.*, 2001). A key region in CooA and related proteins is a long helix, called the C-helix, that connects the DNA-binding and the effector domains, and serves as the dimer interface (Lanzilotta *et al.*, 2000). It is proposed that when CO binds, the heme is displaced into an adjacent cavity and is approached by the C-helix of the opposite subunit. It is suggested that motions trigger the protein conformation change required for DNA binding.

CooA is one of several gas (O_2, CO, NO) sensor proteins that have been identified (Aono, 2003). A mammalian CO-sensing heme protein, called *neuronal PAS domain protein 2*, which serves as a transcriptional regulator of circadian rhythm, recently has been reported (Dioum *et al.*, 2002).

CO Metabolism and the acs System—A CO Metabolizing Machine. The proteins that catalyze the carbonyl (Western) part of the Wood-Ljungdahl pathway are encoded by the *acs* operon (Figure 5). The genes are organized in order of their role in the pathway: MeTr, CFeSP, and CODH/ACS. A Ni-processing protein (AcsF), such as UreE in urease activation (Song *et al.*, 2001), or CooC in the *coo* system (Jeon *et al.*, 2001), and an iron-sulfur protein (orf7) with an unknown role were recently identified (Loke & Lindahl, 2003). This gene cluster is named after ACS, which is unique to organisms that use the Wood-Ljungdahl pathway and, thus, serves as a marker enzyme for this pathway. Some *acs* orthologs are found among various anaerobic Bacteria (acetogens, sulfate reducers, desulfitobacteria) and Archaea (methanogens and

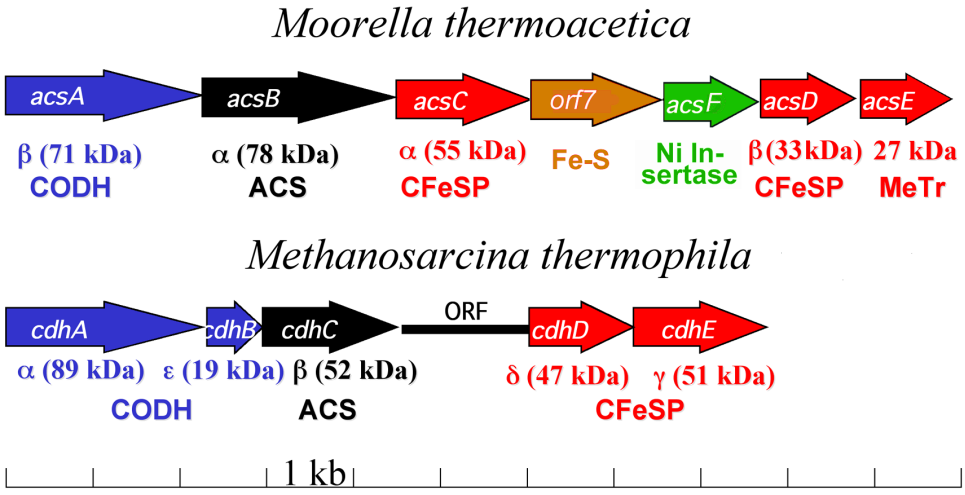

FIG. 5. The acs operon from *M. thermoacetica* is compared with that of *M. thermophila*.

Archaeoglobus). Although the *acs* genes are not regulated by CooA, they are mildly upregulated by CO and strongly regulated at a transcriptional level by nitrate, which is an alternative electron acceptor to CO_2 (Arendsen *et al.*, 1999). The operons in the evolutionarily distant divergent methanogens and acetogens are similar but also show significant differences; for example, there appear to be two extra [4Fe-4S] clusters in the methanogenic CODH, and the arrangement of the genes encoding CODH and ACS appear to be switched relative to the *M. thermoacetica* operon. The methanogenic CODH/ACS (ACDS) has been reviewed recently (Grahame, 2003).

ENZYMES THAT CATALYZE CO OXIDATION

Nomenclature: CODH, ACS, CODH/ACS

The enzymes that catalyze CO oxidation and those that catalyze acetyl-CoA synthesis have sometimes been collectively called "carbon monoxide dehydrogenases" (CODHs). This is problematic for several reasons. CO oxidation and acetyl-CoA synthesis are entirely different in character and would fall into separate categories in the International Enzyme Commission Classification scheme—the oxidoreductase (EC 1.2.x.x) and the lyase (EC 4.2.x.x) classes, respectively. In addition, some CODHs do not contain ACS activity, and ACS can be expressed in the absence of CODH. Names for each activity abound. CODH has been called *CO:acceptor oxidoreductase*, *CO oxidase*, and *CO_2 reductase*.

To avoid confusion, it is important to use names for these enzymes that are congruous with the International Enzyme Commission classification scheme. In 1996, after an extensive discussion among some of the major groups in the field, the following nomenclature was suggested in a review article (Ragsdale & Kumar, 1996). It is suggested that the name *CO dehydrogenase* (CODH) be used as the recommended name and *CO:acceptor oxidoreductase* as the systematic name for the activity that catalyzes CO oxidation to CO_2 or its reverse. This name correctly denotes that this reaction is in the EC1.2 oxidoreductase class. The *acceptor* cannot be further specified because CODH efficiently uses many physiological electron acceptors (ferredoxin, flavodoxin, cytochromes, rubredoxin, etc.) and dye mediators (methylene blue, thionin, methyl viologen, FMN, $FADH_2$, etc.).

It is suggested that the name *acetyl-CoA synthase* (ACS) should be used as the recommended name and *CO:methylated corrinoid iron-sulfur protein:CoA lyase* as the systematic name for the enzyme that assembles acetyl-CoA from enzyme-bound methyl, CO, and CoA groups. Reasons for these choices are described below. To denote the source of the enzyme, the genus and species are included as a prefix in lower-case italicized letters; *e.g.*, for the *Moorella thermoacetica* CODH, the name would be *mt*CODH. For the methanogenic ACS, the name *acetyl-CoA decarbonylase synthase* has often been used; however, it seems unnecessary to use more complicated terms like acetyl-CoA decarbonylase synthase, because it seems redundant to name the reaction in both directions. It also has been argued that both the CODH and ACS activities can be included under the umbrella *CODH*; however, this name disregards the ACS function. The term *acetyl-CoA synthase* has been in use since 1985 and describes the physiological role of the enzyme in acetogenic bacteria and methanogens to catalyze the key activity that defines the autotrophic Wood-Ljungdahl pathway. The recommended systematic name, *CO:methylated corrinoid iron-sulfur protein:CoA lyase*, includes the three substrates for ACS and the enzyme class that designates that the enzyme catalyzes the formation of acetyl-CoA by group elimination reactions in the absence of ATP hydrolysis. Since the reaction is unlike that of other lyase subclasses, ACS should gain the next highest subclass number.

Following from the above discussion, it is recommended that the bifunctional enzyme should be *CO dehydrogenase/acetyl-CoA synthase* or *CODH/ACS*. Neither ACS nor CODH alone would suffice because they describe only the partial reactions. CODH/ACS is preferable to ACS/CODH because CODH precedes ACS in function.

Early Studies of CODH and CODH/ACS

Yagi first identified an enzyme that catalyzes the oxidation of CO to CO_2 (Yagi, 1959). Diekert and Thauer first identified this enzyme in acetogenic bacteria (Diekert & Thauer, 1978), yet it was nearly a decade before CODH was purified to homogeneity, due mainly to its extreme oxygen sensitivity (Ragsdale *et al.*, 1983a). The secret to working with most of the enzymes involved in this pathway is to strictly exclude oxygen. Bacteria must be grown and harvested anaerobically, and every step in the purification and manipulation of the enzymes must be performed in an anaerobic chamber (we use a chamber manufactured by Vacuum Atmospheres that maintains the oxygen level at ~0.2 ppm).

One reason that purification of this enzyme was important was to test the hypothesis that formyl-H_4folate, the first cofactor-bound one-carbon compound in the Wood-Ljungdahl pathway, may be formed by direct transfer of a formate oxidation level intermediate on CODH (called [HCOOH] at the time) to formyl-H_4folate synthetase (Hu *et al.*, 1982). Bypassing formate dehydrogenase in this manner would be advantageous because it would save the ATP required for the synthetase reaction. After CODH was purified to homogeneity and combined with the other purified enzymes of the Wood-Ljungdahl pathway, it was demonstrated that acetyl-CoA synthesis indeed required

formate dehydrogenase, as well as formyl-H_4folate synthetase and CODH/ACS (Ragsdale *et al.*, 1983a).

CODH is one of the few nickel-containing proteins so far discovered in nature. The first indications that CODH contains Ni came from growth studies in which the addition of nickel to the growth medium stimulated CODH activity (Diekert & Thauer, 1980; Diekert *et al.*, 1979). Biochemical evidence was provided when CODH activity and radioactivity were shown to comigrate in polyacrylamide gels of cell extracts of *M. thermoacetica* grown in the presence of the radioactive Ni isotope, ^{63}Ni (Drake *et al.*, 1980). When the *M. thermoacetica* CODH was purified to homogeneity, it appeared to contain 2 mol of nickel per mol of $\alpha\beta$ dimeric enzyme (Ragsdale *et al.*, 1983a), although recent studies demonstrate that the fully active protein contains 3 Ni per dimeric unit (Seravalli *et al.*, 2004). It contains subunits of 77 kDa and 71 kDa (Ragsdale *et al.*, 1983a). CODH/ACS from *M. thermoacetica* was also purified to near homogeneity by Diekert and Ritter(1983) and shown to contain nickel. Diekert and Ritter(1983) also correctly surmised that the protein had an $\alpha_2\beta_2$ structure which was verified later (Xia *et al.*, 1996).

Early Studies of ACS

Many enzymes with the name CODH only catalyze the oxidation of carbon monoxide or its reverse reaction. However, the most important role for the CODH/ACS in acetogenic bacteria is to catalyze the synthesis of acetyl-CoA from a methyl group, CO or CO_2, and CoA. Various roles for CODH in acetate synthesis were suggested, including reduction of an electron carrier or enzyme prosthetic group involved in CO_2 reduction to acetate (Diekert & Thauer, 1978) and formation of an enzyme-bound [HCOOH] group from pyruvate (Drake *et al.*, 1981; Pezacka & Wood, 1984) or CO (Hu *et al.*, 1982). Formation of the C–C bond of the acetyl moiety of acetate was assumed to occur at the cobalt center of a corrinoid or a corrinoid protein. Reasons for this have been summarized (Ragsdale, 1991) and, at this time, the major controversy was whether the synthesis occurred via an acetylcobalt, acetoxycobalt, or a carboxymethylcobalt intermediate.

When Harold Drake was a postdoctor with H. G. Wood, he discovered that a partially purified enzyme fraction catalyzed a remarkable reaction (Equation (6)) in which acetyl-CoA labeled in the carbonyl group became nonradioactive when it was incubated with CO (Hu *et al.*, 1982). This isotope exchange reaction between CO and the carbonyl group of acetyl-CoA offered a simpler system for studying acetyl-CoA synthesis than the entire synthesis reaction, which at the time required five components that catalyzed synthesis of acetyl-CoA from pyruvate, methyltetrahydrofolate, and CoA (Drake *et al.*, 1981), as shown in Figure 1. In the exchange reaction, acetyl-CoA must be disassembled by breakage of the methyl-carbonyl and carbonyl-SCoA bonds and then reassembled, which might involve only the single unknown component—the synthase itself. Based on the dogma of the time, as mentioned above, it was expected that the corrinoid protein, recently isolated in Wood's lab (Hu *et al.*, 1984), would be required for this reaction, since it had been assumed to be the catalyst on which the methyl and acetyl group are assembled. However, the purified CODH was the only catalyst required (Ragsdale & Wood, 1985). Since there were no acceptors of the methyl, CO, or CoA groups of acetyl-CoA in the reaction mixture other than CODH, it was recognized that the synthesis and assembly of acetyl-CoA occur on CODH, that the role of the CFeSP was to transfer the methyl group from methyltetrahydrofolate to CODH, and that a more appropriate name for the enzyme that catalyzes the synthesis of acetyl-CoA from CO, the methyl donor, and CoA is *acetyl-CoA synthase* (Ragsdale & Wood, 1985). Several enzyme-bound organometallic intermediates (M-CO, M-methyl, M-acetyl) were also proposed. What was not clear was whether CODH and ACS activities were catalyzed by the same or by separate active sites (see below). In summary, as described below, it now appears that the assembly of acetyl-CoA does indeed occur on ACS and that the assembly process occurs on metal centers involving organometallic bonds.

$$CO + CH_3{-}{}^{14}CO\text{-}SCoA \rightarrow {}^{14}CO + CH_3{-}CO{-}SCoA \quad [6]$$

The CO Oxidation Catalysts—CODHs

There are three classes of CODH: the Mo-CODH, the Ni-CODH, and the Ni-CODH/ACS.

Mo-CODH. Although the midpoint reduction potential for the CO_2/CO couple (−558 mV, pH 7.0) is very negative, the best electron acceptors for the Mo-CODH have midpoint potentials between +0.011 V and 0.043 V, which contrasts with the Ni-CODHs that reduce a variety of high- and low-potential electron acceptors. The CODHs from carboxydotrophs also can oxidize NADH, an activity associated with all known Mo hydroxylases. Unlike the Ni-containing CODHs, the Mo enzymes are not oxygen sensitive.

The mesophilic enzyme from *Oligotropha carboxydovorans* and the thermophilic enzyme from *Oligotropha thermocarboxydovorans* have similar molecular masses (230,000–310,000) and $(\alpha\beta\gamma)_2$ structures (Meyer *et al.*, 1986). The carboxydotrophic CODH is encoded by plasmid-borne genes (Black *et al.*, 1990; Hugendieck & Meyer, 1992; Meyer *et al.*, 1990) that have been cloned and sequenced (Pearson *et al.*, 1994; Schubel *et al.*, 1995).

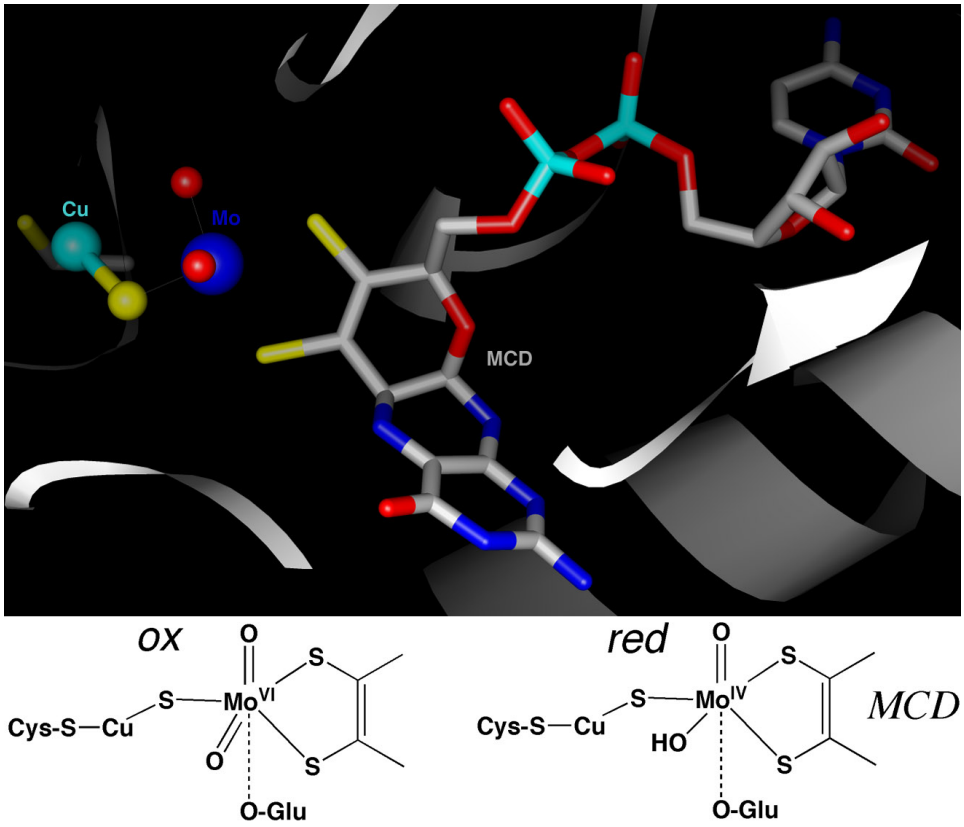

FIG. 6. The active site of the Mo-CODH. MCD is molybdopterin cytosine dinucleotide.

The active site contains a Cu linked to a Mo-pterin, molybdopterin cytosine dinucleotide (MCD) (Figure 6) (Gnida *et al.*, 2003; Johnson *et al.*, 1990). It was thought that Se was present in the active site, even based on the first crystal structure of the enzyme (Dobbek *et al.*, 1999); however this has been disproven (Dobbek *et al.*, 2002; Gnida *et al.*, 2003). These CODHs also contain 2 mol of FAD and 8 Fe and 8 acid-labile sulfide, which are present as [2Fe-2S] centers (Bray *et al.*, 1983) and are involved in electron transfer to the catalytic Mo-pterin center (Meyer *et al.*, 1993). Evidence that Mo is at the active site of CO binding is based on inhibition of enzyme activity by methanol, which traps Mo in the V state, the requirement of Mo for growth on CO, but not for heterotrophic growth, and inhibition of CO-dependent growth by the Mo antagonist, tungstate (Meyer & Schlegel, 1983). Meyer recently proposed that CO binds to the Cu site (Gnida *et al.*, 2003).

The Ni-CODHs. The CODHs from *R. rubrum*, *C. hydrogenoformans*, and *M. thermoacetica* have been most extensively studied, and structures are known for each of these proteins. The structures of the three enzymes are very similar, and all ligands at the active site, as well as some residues proposed to facilitate acid-base chemistry at the active site, are conserved (Table 1). The *R. rubrum* and *C. hydrogenoformans* CODHs offer the advantage that they lack the ACS subunit, allowing focus on CODH alone. In addition, for *R. rubrum* a Ni-deficient protein containing all the Fe sites in the holoenzyme has been isolated (Ensign *et al.*, 1989).

The CODH mechanism proposed here (Figure 7) and discussed in detail below is analogous to that of the water-gas shift reaction (Figure 8). The individual steps are discussed below. The key common intermediates include a metal-bound carbonyl, a metal bound hydroxide ion, and a metal carboxylate formed by attack of the M-OH on M-CO. Elimination of CO_2 either leaves a metal-hydride or a two-electron-reduced metal center and a proton. In the CODH mechanism, It is proposed that the metal center becomes reduced by two electrons; however, CODHs have a weak CO-dependent hydrogen evolution activity that would be consistent with a metal-hydride intermediate (Bhatnagar *et al.*, 1987; Menon & Ragsdale, 1996; Santiago & Meyer, 1996b). Regardless, the key difference between the CODH mechanism and the water gas reaction is that, in the enzyme, electron transfer is very rapid relative to H_2 evolution because of the placement of the B and D clusters as electron acceptors, like a wire, between the C-cluster and the site at which external electron carriers bind.

TABLE 1
Key amino acid residues among the CODHs

Organism* (acc #)	B-Cluster	D-Cluster	C-Cluster	A-Cluster
		A. Ligands to the metal clusters in CODH and CODH/ACS		
Rr (1JQK)	C50, C53, C58, C72	C41, C49	C300, C338, H265, C451, C481, C531	
Ch (1JJY)	C48, C51, C56, C70	C39, C47	C295, C333, H261, C446, C476, C526	
Mt (1OAO,1MJG)	C68, C71, C76, C90	C59, C67	C317, C355, H283, C470, C500, C550	FeS: C506, C509, C518, C528 Ni_P: C509, C595, C597 Ni_D: S of C595, C597 & backbone N of G596, C597

Organism* (acc #)	Histidine tunnel	Acid base chemistry
	B. Potential catalytic residues for CO oxidation	
Rr (1JQK)	H95, H98, H101	K568, H95, D223, W575
Ch (1JJY)	H93, H96, H99, H102	K563, H93, D219, W570
Mt (1OAO, 1MJG)	H113, H116, H119, H122	K587, H113, D241, W594

*Rr, *R. rubrum*; Ch, *C. hydrogenoformans* CODHII; Mt, *M. thermoacetica.*

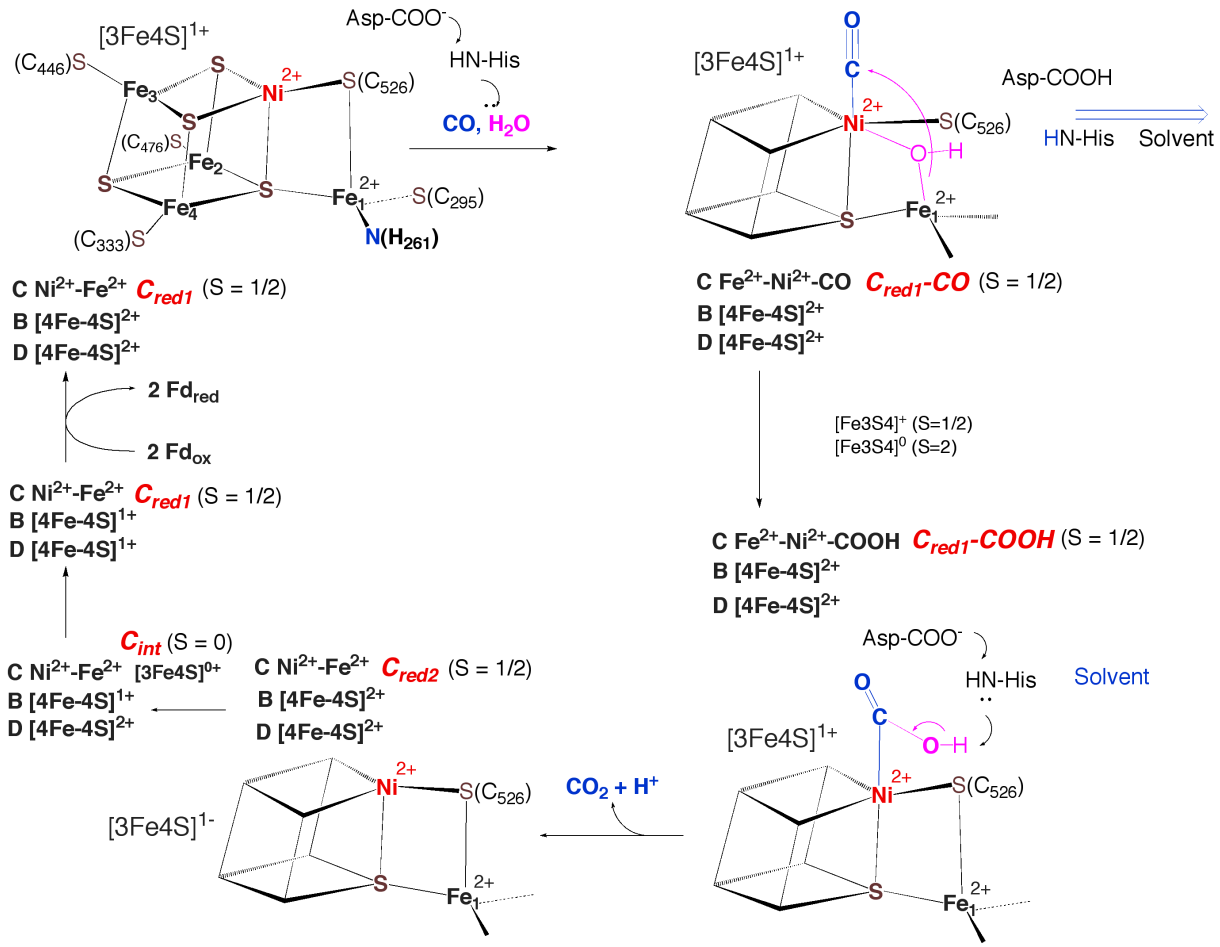

FIG. 7. Proposed CODH mechanism. Cred1, Cint, and Cred2 are different states of the C Cluster. Cox, which is not shown, is a diamagnetic state (Ni^{2+}-Fe^{3+}) that requires 1 electron reduction to the active Cred1 state.

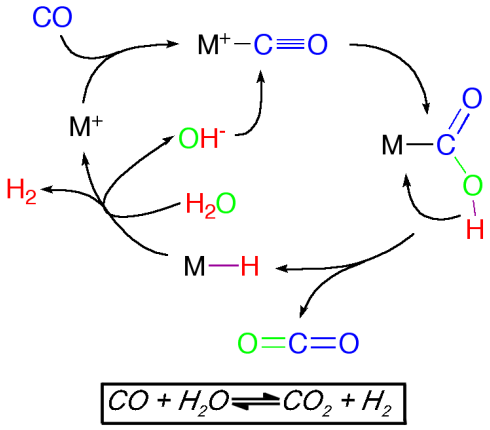

FIG. 8. The water-gas shift reaction, an organometallic reaction sequence.

Structure of Ni-CODH. The X-ray crystal structure of CODH (Darnault *et al.*, 2003; Dobbek *et al.*, 2001; Doukov *et al.*, 2002; Drennan *et al.*, 2001) reveals a mushroom-shaped homodimeric enzyme containing five metal clusters (Clusters B, C, and D), as shown in the center of this figure of the CODH/ACS from *M. thermoacetica* (Figure 9). In this bifunctional enzyme, the CODH subunits (cyan and blue) contain the catalytic site of CO oxidation (the C-Cluster) and the redox centers (Clusters B and D) that transfer electrons to and from the C-Cluster. The orange and green ACS subunits at the periphery are discussed later. Buried 18 Å below the surface in each CODH subunit is a C-Cluster, which is a Ni-4Fe-5S (or Ni-4Fe-4S) cluster that can be viewed as a [3Fe-4S] cluster bridged to a heterobinuclear NiFe cluster. Rees (2002) noted that the structural motif for binding the C-Cluster, a four-stranded, parallel β-sheet surrounded by α-helices, is also found in other complex FeS metalloclusters, like nitrogenase and the Fe-only hydrogenase. The protein ligands to these clusters are found in loops positioned between two β strands. Converging just above the Ni center in the C-Cluster are a hydrophobic channel, proposed to deliver CO to the Ni center, and a solvent channel containing over 40 water molecules to deliver the other substrate, water.

Electrons generated during CO oxidation are transferred to a wire consisting of the B- and the D-Clusters, as shown in the CODH/ACS structure. While each CODH subunit contains a B-Cluster, the D-Cluster is shared by the two CODH subunits, similar to the FeS cluster in the iron protein of nitrogenase. Interestingly, it is the B-Cluster of the adjacent subunit that is suitably positioned to mediate the electron transfer between the C— and D—Clusters. The D—Cluster, which is nearest to the molecular surface, is likely to mediate electron transfer between CODH and the terminal electron acceptor (ferredoxin, flavodoxin, etc.). The reduced electron acceptors then couple to other energy, requiring cellular processes.

The same sequence of reactions just described run in reverse in CODH/ACS, which functions to convert CO_2 to acetyl-CoA, *i.e.*, here the CODH functions to produce CO, water from protons, and CO_2. Although the alpha carbon backbone of the CODH subunits from *M. thermoacetica*, *R. rubrum*, and *C. hydrogenoformans* overlay with a 0.8–1.0 Å root-mean-square deviation, two key alterations in CODH have occurred in the CODH/ACS class of proteins. It appears that the CO oxidation activity has been attenuated, with specific activities of 20,000 U/mg (per

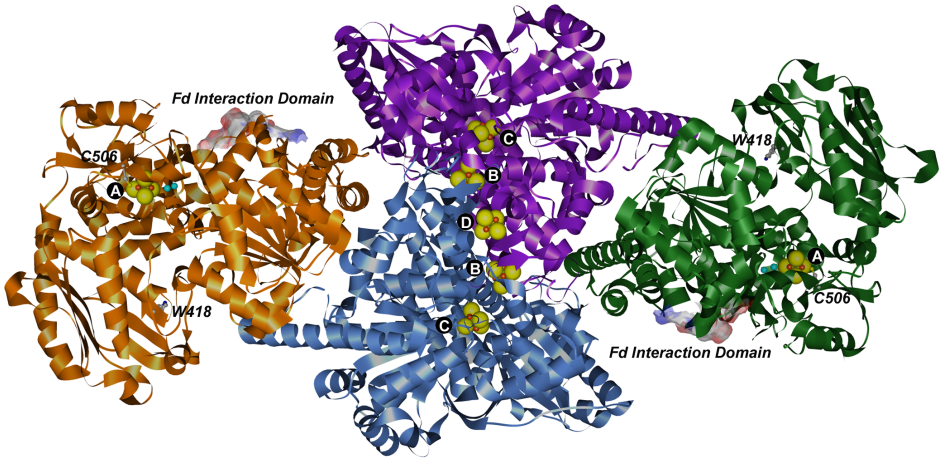

FIG. 9. CODH/ACS structure. The purple and cornflower blue subunits in the center are ribbon drawings of CODH. The metal clusters are shown as spheres and labeled. The orange and forest green subunits at the periphery are ACS. C506 of ACS was identified as a site for interaction with the CFeSP. Residues 229–239 of ACS were identified as a site that interacts with ferredoxin. Trp418 of ACS was shown to interact with CoA. Generated using Chimera from 1MSG.

monomeric unit, kcat of ~22,000 s^{-1}) in the CODH-only versus 600 U/mg (per heterodimeric unit, kcat ~ 1500 s^{-1}) in CODH/ACS. Furthermore, the hydrophobic channel described above has undergone a change, perhaps a redirection, as a 140 Å leak-free channel is carved into the ACS subunit to deliver CO generated at the CODH-active site to the A-Cluster (described in detail below).

Based on spectroscopic studies of CODH, the C-Cluster was interpreted to contain a high spin (S = 1) Ni^{2+} site connected through a bridging ligand to a $[4Fe\text{-}4S]^{2+/1+}$ cluster (Hu *et al.*, 1996). The inability to detect a Ni-Fe interaction by X-ray absorption spectroscopy (XAS) was a major reason for dismissing the possibility that Ni could be part of the cubane (Tan *et al.*, 1992). However, the high resolution (1.6 Å) X-ray structure of the as-isolated CODH from *C. hydrogenoformans* (Dobbek *et al.*, 2001) revealed that the Ni ion is indeed incorporated in a $NiFe_4S_4$ cubane cluster, coordinated by four S atoms in a slightly distorted square planar geometry, and bridged to four Fe atoms through inorganic sulfide ligands with Ni and Fe distances ranging from 2.8 to 3.7 Å (Figure 10). In the 2.8 Å structure of *R. rubrum* CODH (Drennan *et al.*, 2001) and the 1.9 Å structure of CODH/ACS (T.I. Doukov, C.L. Drennan, J. Seravalli, and S.W. Ragsdale, unpublished results; Doukov *et al.*, 2002), the Ni site in the C-Cluster also is part of the cube and adopts a distorted five-coordinate geometry with 4 S and another unidentified ligand, and the Ni and Fe distances vary from 2.6 to 2.8 Å.

XAS of the *C. hydrogenoformans* CODH was used to assess these apparent discrepancies in ligand binding and Ni-Fe distances (Gu *et al.*, 2004). The X-ray absorption K-edge energy (8340 eV) is consistent with a Ni^{2+} assignment and, upon reduction with CO, the Ni K-edge changes only slightly, implying that the Ni remains in (or quickly returns to) the 2+ state upon reduction (Gu *et al.*, 2004). The Ni extended X-ray absorption fine structure (EXAFS) spectrum of the as-isolated protein can be simulated with 4 Ni-S interactions at 2.20 Å without a Ni-Fe interaction. Simulation of the XAS spectra according to the crystal structure of the dithionite-treated enzymes indicates that the Ni-Fe vector was not detected by XAS because the distances are long and because heterogeneity in Ni-Fe vectors resulted in a destructive interference that veiled this interaction. Thus, the XAS-derived structure of the C-Cluster in the as-isolated enzyme is similar to the crystal structure of the dithionite-treated enzyme (Dobbek *et al.*, 2001). When CODH is treated with CO or the strong reductant Ti(III)citrate, the Ni site becomes more tetrahedral as the average Ni-S distance expands to 2.25 Å and a new strong feature appears at 2.7 Å (see arrow) that is consistent with a Ni-Fe interaction. The changes between the two forms suggest that CO treatment causes the Ni

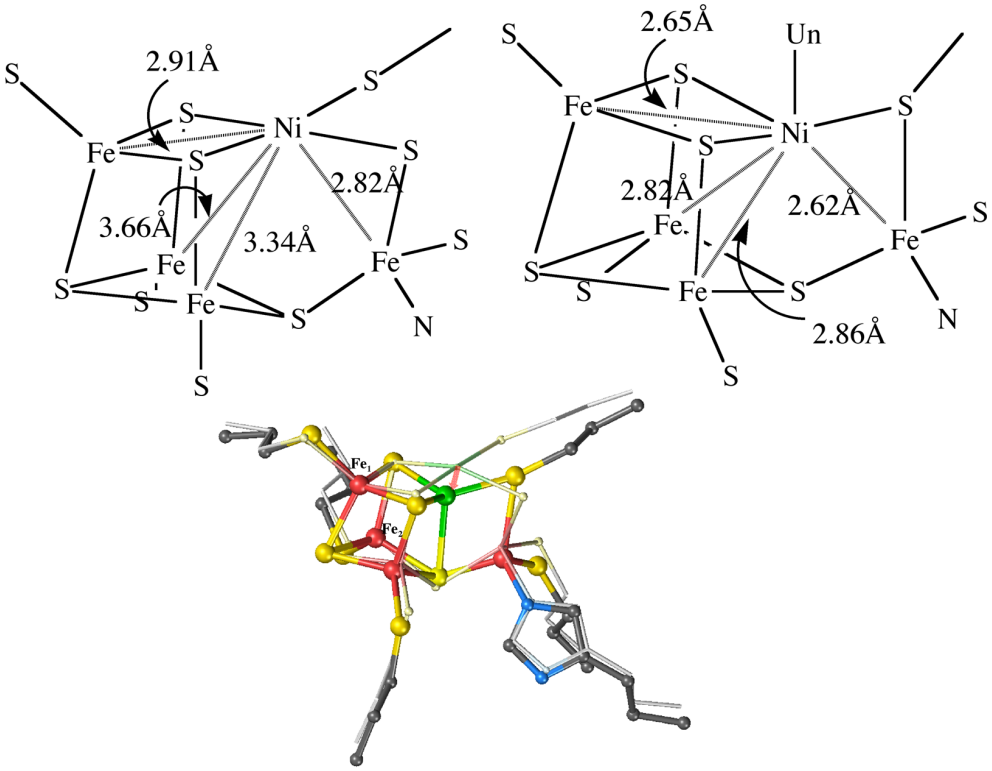

FIG. 10. Comparison of the C-Cluster structures of *C. hydrogenoformans* (left) and *R. rubrum* (right). Reprinted with permission from Gu *et al.*, 2004.

in the C-Cluster to move ~1 Å (shown by the red arrow), adopting a more tetrahedral geometry. These results (Gu *et al.*, 2004) rationalize some of the apparent differences between the crystal structures of the *C. hydrogenoformans* (Dobbek *et al.*, 2001) and the *R. rubrum* (Drennan *et al.*, 2001) proteins. It is unclear why the XAS spectra of as-isolated enzyme match the crystal structure of the dithionite-treated enzyme; perhaps the dithionite, an unstable reductant, underwent oxidation during the crystallization procedure.

Substrate access and binding to the active site. The first step in the CODH reaction is the binding of substrates, CO and H_2O or CO_2 and protons. Dobbek *et al.* (2001) described a hydrophobic CO channel in the COOH-terminal domain of ACS and a hydrophilic, positively charged water channel that connects the surface and the C-Cluster in the *C. hydrogenoformans* CODH II (described above in the structure section).

An open coordination site above Ni in the C-Cluster was proposed to be the site of CO binding (Dobbek *et al.*, 2001; Drennan *et al.*, 2001). This hypothesis is consistent with recent infrared (IR) studies of the *M. thermoacetica* CODH-CO complex in which multiple IR bands at 2078, 2044, 1970, 1959, and 1901 cm^{-1} were observed and attributed to Ni-CO in different states of the C-Cluster (see Figure 16 below; Chen *et al.*, 2003). All IR bands attributed to M-CO species disappear in a time-dependent fashion as bands for metal-carboxylates (1724 and 1741 cm^{-1}) and CO_2 (2278 cm^{-1}in the ^{13}CO sample) appear, which is consistent with enzyme-catalyzed CO oxidation during the IR experiments. No M-CO bands are detected in as-isolated CODH/ACS, suggesting that, unlike the NiFe (Bagley *et al.*, 1995; Happe *et al.*, 1997) or Fe-only (Chen *et al.*, 2002) hydrogenases, neither CODH nor ACS contain intrinsic M-CO ligands.

Catalysis of CO oxidation. What is the mechanism by which an enzyme like the *C. hydrogenoformans* CODH can catalyze the oxidation of CO to CO_2 with a turnover number of 39,000 mol CO per mol enzyme per second and a k_{cat}/K_m of over 10^9 $M^{-1}s^{-1}$ (Svetlitchnyi *et al.*, 2001)? Furthermore, these enzymes can catalyze the reduction of CO_2 to CO with a turnover number of 10 s^{-1} (Kumar *et al.*, 1994) without imposing an overpotential (a potential above that required to reach ox/red equilibrium), while the catalysts used for industrial CO_2 activation and reduction require an overpotential of about a volt. The C-cluster of CODH is the active site for the oxidation of CO to CO_2. This conclusion is based on rapid kinetic studies, which show that the electron paramagnetic resonance (EPR) spectra of the C-Cluster change from the Cred1 to the Cred2 states (below) at rates commensurate with the rate of CO oxidation (Kumar *et al.*, 1993). In addition, cyanide, which is a competitive inhibitor of CO oxidation with respect to CO, binds specifically to the C-Cluster (Anderson *et al.*, 1993).

As shown in Figure 7, the catalytic cycle involves two half reactions. The first involves the chemistry of CO oxidation and reduction of the metal clusters (B, C, and D). The second half of the cycle is electron transfer from the reduced enzyme (C_{red1}, B_{red}, D_{red}) to ferredoxin. The C-Cluster has four redox states: C_{ox}, C_{red1}, C_{int}, and C_{red2}. C_{red1} and C_{red2} can be observed by EPR spectroscopy. The midpoint potential of the C_{ox}/C_{red1} couple is approximately −200 mV, whereas that for the formation of C_{red2} is ~−530 mV (Lindahl *et al.*, 1990a). It is not known whether C_{red2} is at the same redox state as C_{red1} or is two-electrons more reduced. C_{red1} appears to be the state that reacts with CO, since it disappears at the rate that C_{red2} is formed (Kumar *et al.*, 1993) and undergoes redox changes at a potential that matches that for catalysis (Feng & Lindahl, 2004). Earlier experiments had indicated a mismatch between the potentials for C-Cluster reduction and catalysis (Heo *et al.*, 2001a, 2001b). The Cred1 state, which has a net electronic spin of 1/2 since it exhibits an EPR spectrum in the g = 2.0 region, is described as a $[3Fe\text{-}4S]^{1+}$ cluster bridged to a binuclear Ni^{2+}/Fe^{2+} site. Another possibility is that the 3Fe cluster has a net 1- core charge (Lindahl, 2002). Apparently, as described below, the Cred2 state also can bind CO (Seravalli *et al.*, 1997).

Figure 7 shows CO and water binding to CODH and, based on electron nuclear double resonance (ENDOR) studies, it is likely that the water molecule binds to a metal center, presumably Fe (DeRose *et al.*, 1998). The pKa of bound water would be significantly lowered and facilitate formation of an active hydroxide, as has been shown for a number of hydrolases, such as carbonic anhydrase (Bertini & Luchinat, 1994). A similar mechanism accounts for activation of metal-bound thiolates in methyltransferases (Gencic *et al.*, 2001; Matthews & Goulding, 1997; Warthen *et al.*, 2001).The active metal-hydroxide is then proposed to attack the M-CO complex. Several basic residues near the C-Cluster, including Lys563, His93, and His261, and several histidine residues were proposed to participate in these acid-base reactions (Figure 11) (Dobbek *et al.*, 2001; Drennan *et al.*, 2001). The His residues are located on sequential turns of a helix, forming a His tunnel that begins near the C-Cluster and leads to the surface of the protein (shown in gold mesh). The His tunnel is proposed to deliver protons that are liberated during the reaction to the solvent.

Conversion of the metal-carboxylate to CO_2 would reduce the C-Cluster by two electrons and form the C_{red2} state, which is represented here as a 3Fe cluster in the 1- state and Ni and Fe still in the 2+ states. A Ni^0 state has also been considered; in this case, the 3Fe cluster would not undergo redox changes (Lindahl, 2002). It is considered

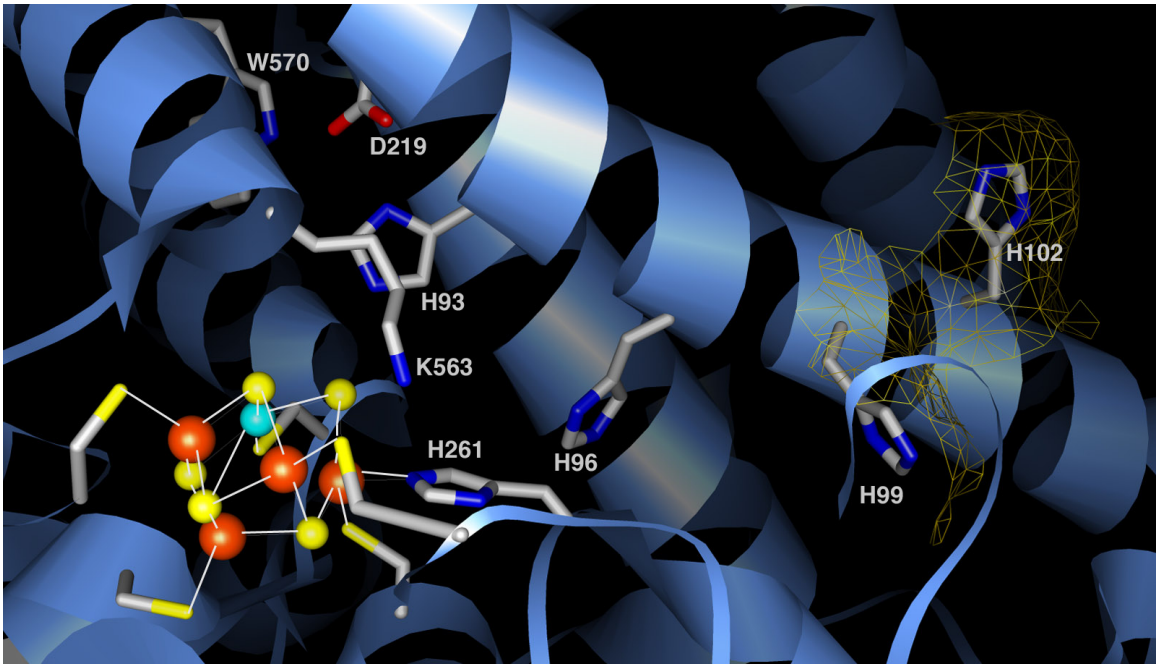

FIG. 11. Cluster C and potential acid base chemistry. Fe, S, and Ni atoms are colored orange, yellow, and cyan, respectively. The surface from H99 to H102 is shown as gold mesh. From 1JJY using Chimera. The numbering is based on the *C. hydrogenoformans* sequence.

that reduction of the B and D clusters would occur one electron at a time, which would leave a diamagnetic Cint state as an intermediate before Cred1 is reformed.

The catalytic cycle involves two half reactions. The first involves the chemistry of CO oxidation and reduction of the metal clusters (B, C, and D). The second half of the cycle is electron transfer from the reduced enzyme (C_{red1}, B_{red}, D_{red}) to ferredoxin. Cluster C of CODH/ACS undergoes changes in its EPR signal as it binds CO at near diffusion-controlled rates ($k = 2 \times 10^8$ $M^{-1}s^{-1}$) and delivers electrons to Cluster B (3,000 s^{-1}) at rates that are catalytically relevant for CO oxidation (k_{cat} = 2000 s^{-1} and k_{cat}/K_m^{CO} is 2×10^7 M^{-1} s^{-1} at 55°C; Kumar *et al.*, 1993). At high CO concentrations, the rate-limiting step in CO oxidation is the second half reaction, oxidation of the reduced enzyme by the electron acceptor; whereas at low CO concentrations, it is the intramolecular electron transfer from the C-Cluster to the B-Cluster (Kumar *et al.*, 1993; Seravalli *et al.*, 1997). The intramolecular electron transfer reaction is also rate limiting when CODH is rapidly mixed with CO during single turnover kinetics in the absence of electron carriers.

The wire. Oxidation of CO is coupled to the one-electron reduction of the B-Cluster and another redox center in the protein, which has been called *X* and may be the D-Cluster. So far, redox changes in the D-Cluster have not been observed. The B- and D-Clusters form an intramolecular wire that connects the catalytic C-Cluster to external electron acceptors/donors (Figure 12). The distance between the nearest Fe atoms of the B- and C-Clusters is ca. 11 Å, while only 8 Å separate the nearest sulfur atoms of cysteine residues 470 and 71. Similarly, between the

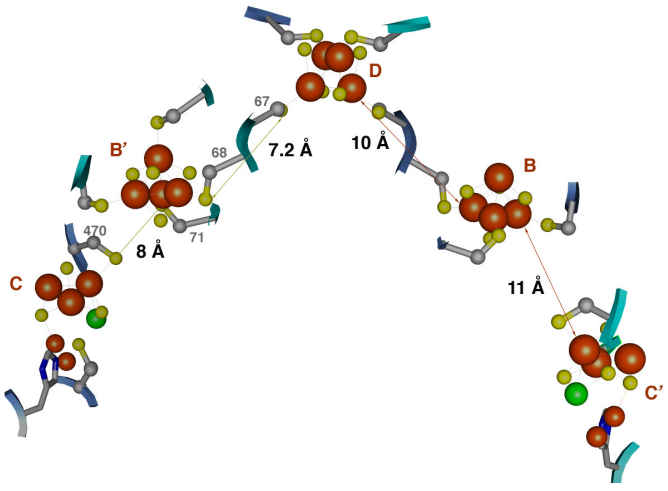

FIG. 12. Metal clusters in CODH. The loops on which the amino acid side chains that ligate the clusters are colored separately to indicate that electron transfer must occur between the C-Cluster of one subunit and the B-Cluster of the other. The distance between the C and B-Clusters of a single subunit is 28 Å, which is too long for effective electron transfer.

nearest sulfur atoms of the B- and D-Clusters, the distance is only 7 Å (sidechains of Cys67 and Cys68), while the nearest Fe atoms are ca. 11 Å apart. These distances would allow rapid electron transfer (Page *et al.*, 1999). The reduction of "X" is required to balance the electron transfer reaction and to explain the rapid reaction kinetics and the potentiometric titrations of CODH with CO and other reductants (Seravalli *et al.*, 2002). Thus, at the end of this reductive half of the catalytic cycle, CODH has undergone a four-electron reduction. Closure of the catalytic cycle involves coupling the intramolecular wire to an external electron carrier protein.

Cluster D is partially surface exposed and is in suitable position to mediate electron transfer between the B-Cluster and the many external mediators to which CODH can couple. This enzyme can efficiently transfer electrons to rubredoxin, methylene blue, a 4Fe and 8Fe ferredoxin, benzyl viologen, flavodoxin, and methyl viologen, with the rates decreasing in that order (Ragsdale *et al.*, 1983a). As an electron acceptor, CODH efficiently accepts electrons directly from pyruvate ferredoxin oxidoreductase ($k_{cat}/K_m = 7 \times 10^7\ M^{-1}\ s^{-1}$, similar to the specificity for ferredoxin; Menon & Ragsdale, 1996a). It also donates electrons to an Fe-only hydrogenase (Ragsdale & Ljungdahl, 1984a), the corrinoid iron-sulfur protein (Ragsdale *et al.*, 1987), low-potential artificial acceptors like triquat, and very high-potential acceptors like cytochrome c.

When CO is produced from CO_2 by CODH/ACS by reversal of these reaction steps, a reduced electron donor transfers electrons to Clusters B and D, which reduce Cluster C. The C_{red2} state then undergoes oxidation, reducing CO_2 to CO.

CO CHANNELING

In CODH/ACS, the CO that is generated by the steps just described is channeled to ACS for acetyl-CoA synthesis.

Gas Channels in Proteins

There are few examples of gas channels in proteins. Proteins that have been proposed to transport ammonia (Soupene *et al.*, 2002a) and CO_2 (Soupene *et al.*, 2002b) have been reported.

Gases can occupy any hydrophobic cavities in proteins. NMR spectroscopy has been used to identify hydrophobic cavities in lysozyme by measuring the dipole-dipole interactions between water protons and the protons of several gases (H_2, CH_4, ethylene, or cyclopropane; Otting *et al.*, 1997). Channels are also located in proteins by X-ray crystallography (Schiltz *et al.*, 2003). Hydrogenase and CODH crystals have been treated with Xe under pressure and flash frozen to locate the channels (Darnault *et al.*, 2003; Montet *et al.*, 1997). The noble gas serves as a heavy atom reporter for the gas channel and can be used to help in phasing of the structure. Since any cavity in the protein can be occupied by the gas, in proteins like hydrogenase and CODH/ACS that use gases, the key issue appears to be directing the gas to and from a particular active site and preventing it from diffusing into nonproductive pathways.

Biochemical Evidence for a CO Channel

Biochemical results strongly indicate that in CODH/ACS, CO derived from CO_2 migrates from the C-Cluster through a channel in the interior of the protein to the A-Cluster in the ACS subunit (Figure 13) (Maynard & Lindahl, 1999; Seravalli & Ragsdale, 2000). In one set of experiments, the effect of unlabeled CO on incorporation of label from $^{14}CO_2$ into acetyl-CoA was measured. If the CO is released from the protein before binding to the A-Cluster, it would equilibrate with CO in solution and decrease the incorporation of label from $^{14}CO_2$. However, even saturating levels of CO did not decrease the incorporation of CO_2-derived CO into the carbonyl group of acetyl-CoA (Seravalli & Ragsdale, 2000). Furthermore, the rate of acetyl-CoA synthesis from CO_2, CH_3-H_4folate, and CoA was significantly faster than the rate with CO, CH_3-H_4folate, and CoA (Maynard & Lindahl, 1999). In addition, hemoglobin, which tightly binds CO, only partially inhibits the synthesis of acetyl-CoA from CH_3-H_4folate, CoA and pyruvate (Menon & Ragsdale, 1996a). Accordingly, no inhibition by hemoglobin was observed in the synthesis from CO_2 (Maynard & Lindahl, 1999). Hemoglobin and myoglobin also only partially inhibit the exchange reaction between CO_2 and acetyl-CoA (Seravalli & Ragsdale, 2000).

These results provide strong evidence for the existence of a CO channel between the C-Cluster in the CODH subunit and the A-Cluster in the ACS subunit. It has been proposed that this channel may be involved in synchronizing cluster activities, increasing the local concentration of CO at the A-cluster, and/or directing CO to a productive rather than inhibitory binding site on the A-cluster (Doukov *et al.*, 2002). Such a channel would tightly couple

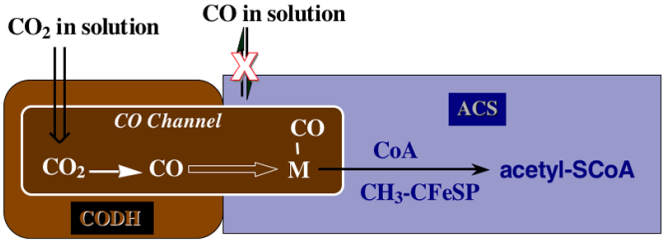

FIG. 13. CO channel in CODH/ACS. This figure shows that CO derived from CO_2 during synthesis of acetyl-CoA does not equilibrate with solvent, but remains sequestered within a channel that connects the C-Cluster in CODH to the A-Cluster in ACS.

CO production and utilization and help explain why very low levels of CO escape into the growth medium of acetogenic bacteria. Since CO is a rich electron donor, it is important that microbes sequester the CO and ensure that the energy devoted to the synthesis of CO is not lost. The channel would also protect aerobic organisms that harbor the microbes by preventing CO from escaping into solution and maintaining CO below toxic levels.

Atomic Resolution Structure of the Channel

A 67 Å hydrophobic channel that connects the A- and C-Clusters was located using the program CAVENV (Doukov *et al.*, 2002). Since this channel connects the C- and A-Clusters of both pairs of subunits, its total length is ~138 Å. This channel has been observed by X-ray diffraction studies of Xe-pressurized crystals (Darnault *et al.*, 2003). Dobbek *et al*. (2001) had identified one end of a hydrophobic channel just above the Ni site of the C-Cluster of CODH. This would be the beginning of the CO channel for the CODH/ACS. Recent Xe studies demonstrate that the other end of the channel is within bonding distance of the proximal Ni site of the A-Cluster (T.I. Doukov, C.L. Drennan, J. Seravalli, and S.W. Ragsdale, unpublished data).

As described below, there is a major conformational change in ACS that exposes the A-Cluster to solvent, which could compromise the integrity of the channel. However, the open channel observed in one state (the closed state, see below) of the enzyme is closed by movement of a helix (residues 143–148 of the Mt enzyme) when the A-Cluster is exposed to solvent (Darnault *et al.*, 2003).

One might ask why nature has placed the A- and C-Clusters so far apart. It seems that a CODH/ACS docking site near the A-Cluster would make the channel unnecessary. Perhaps nature has placed the A-Cluster and C-Cluster (or any of the CODH clusters) far enough apart that oxidation of the A-Cluster is not feasible under physiological conditions. This would isolate the A-Cluster from the redox chemistry associated with CO oxidation and help maintain the Ni_P site in its catalytically active reduced form.

CO UTILIZATION: CELL CARBON FROM CO

ACS

ACS Structure

Overall structure of ACS. The orange and green ACS subunits shown in Figure 9 consist of three domains that are connected by long flexible loops. Residues 1–312 in the first domain form a Rossman (six-stranded α/β) fold and form the interface with CODH. Interestingly, this domain is missing in the methanogenic cdhC (the beta subunit), which contains the A-Cluster. This domain also contains a ferredoxin-binding region (shown in Figure 9 with the purple surface), which was identified by crosslinking the ferredoxin-CODH/ACS complex, cleaving with cyanogen bromide, and sequencing (Shanmugasundaram & Wood, 1992). Residues in the Fd-binding domain are ca. 10 Å from the A-Cluster; thus, a ferredoxin–ACS complex could be involved in activation of the A-Cluster and in any internal electron transfer reactions that occur during the ACS reaction. The second domain (residues 313–478) contains Trp418 close to six Arg residues. Based on two experiments, Arg residues have been implicated in binding CoA. The fluorescence of Trp418 is quenched upon CoA binding (Shanmugasundaram *et al.*, 1988), and phenylglyoxal, which is a rather specific Arg modification reagent, inhibits CoA binding (Ragsdale & Wood, 1985). The third domain (residues 479–729) contains the ligands to the A-Cluster (see Table 1). Cys506 was identified to form a disulfide bond with a thiol group on the CFeSP (Shanmugasundaram *et al.*, 1993).

Although all the CODH structures are highly similar, the ACS subunits in the two *M. thermoacetica* crystal structures exhibit different conformations. In Figure 9, the orange subunit is in an open conformation in which the A-Cluster is more solvent exposed, while the green ACS subunit is in the closed conformation. Except for the position of one helix, the N-terminal domains of the open and closed structures overlay; however, the second and third domains in the two conformations are rotated as a rigid body by ca. 50°. This rotation explains two important aspects of the ACS mechanism. The first major issue relates to the need to interface ACS with the CFeSP. The methyl group transfer from the CH_3–Co-corrinoid to the Ni of the A-cluster appears to occur by an S_N2 mechanism (Menon & Ragsdale, 1998, 1999), which requires the Co-CH_3 to be positioned directly above the Ni_P in the A-Cluster. In the closed state, there is insufficient space for B_{12} or the CFeSP to interact with the A-Cluster. However, in the open state, the exposed A-Cluster is more accessible to allow docking of the CFeSP and facilitate transfer of the methyl group from Co to the A-Cluster. Thus, a major conformational change appears to be coordinated with each catalytic cycle. However, solvent exposure of the A-Cluster to solvent presents a problem: CO must be retained in the channel until it binds to the metal site to undergo condensation with the methyl and CoA groups. This is accomplished by a closure of the CO channel when the protein adopts the open conformation by the movement of a helix in the N-terminal domain. When ACS readopts the closed conformation, this helix moves again to open the channel.

Active site structure—the A-Cluster. This active center of ACS, the A-Cluster was the first published example of a NiFeS cluster (Ragsdale *et al.*, 1985). It consists of a [4Fe-4S] cluster bridged to a Ni site (Ni_p) that is thiolate

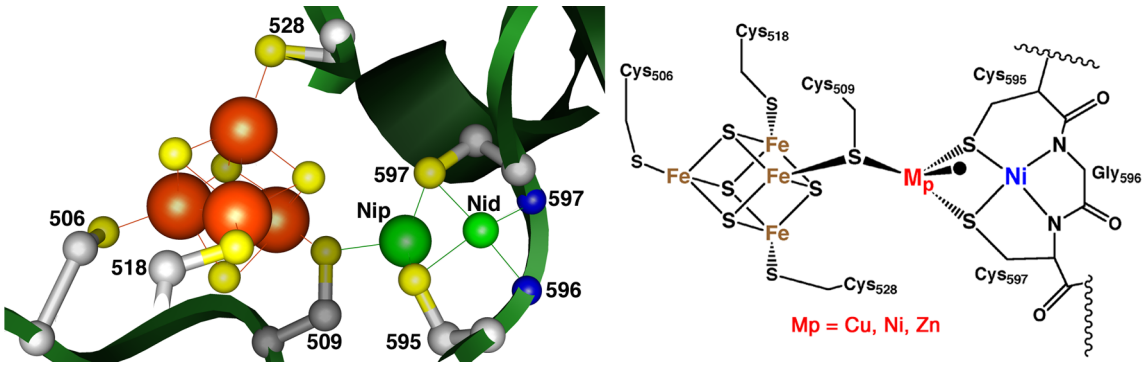

FIG. 14. A-Cluster of ACS. Ni_d and Ni_p are the distal and proximal nickels. Fe atoms are shown in orange-red, sulfurs in yellow, Ni in green. The loops contain the side chains that serve as ligands. This closeup is from the green subunit shown in the overall CODH/ACS structure and was generated using Chimera from 1OAO after replacing Zn with Ni.

bridged to another Ni ion in a thiolato- and carboxamido-type N_2S_2 coordination environment (Figure 14, Table 1) (Doukov *et al.*, 2002). Thus, one can describe the A-Cluster as a binuclear NiNi center bridged to a [4Fe4S] cluster. A proposal that Cu is a component of active ACS (Doukov *et al.*, 2002; Seravalli *et al.*, 2003), met with immediate criticism (Bramlett *et al.*, 2003; Darnault *et al.*, 2003; Gencic & Grahame, 2003; Hausinger, 2003) based first on studies on the methanogenic ACS (ACDS) from the Grahame laboratory (Gencic & Grahame, 2003). Metal analyses on recombinant and native methanogen ACDS β subunit showed insignificant levels of copper, and an Fe:Ni ratio of 2:1 consistent with 2Ni per [4Fe-4S] cluster. Using apo-ACDS β subunit, Grahame and Gencic showed that a reconstituted Ni–Ni form of the A-Cluster had activity, while a Cu–Cu form did not. Based on metal reconstitution experiments (using Cu^{2+} and Ni) with the acetogenic enzyme, Fontecilla-Camps and Lindahl concluded that the CuNi form of ACS is inactive and the NiNi form is active (Bramlett *et al.*, 2003). However, the above experiments were not unambiguous since activity of the CuNi methanogenic enzyme was not tested (Gencic & Grahame, 2003) and, with the acetogenic CODH/ACS, added Cu^{2+} inhibited both ACS activity of the A-Cluster and CODH activity at the C-Cluster (Bramlett *et al.*, 2003). The most serious questions about the activity of the CuNi form of the enzyme were based on the demonstration that removal of Ni by o-phenanthroline (ophen) results in loss of ACS activity and that readdition of Ni restores activity (Russell *et al.*, 1998; Shin & Lindahl, 1992); however, since the presence of Cu in CODH/ACS was unknown at that time, the effect of Cu addition was not addressed.

Determining unambiguously whether the CuNi or the NiNi enzyme is active proved to be challenging. The initial proposal that Cu was an active component of ACS was based on a positive correlation between Cu and activity with samples, where metal occupancy was in the range 1.6–2.3 Ni per $\alpha\beta$ and 0.25–0.96 Cu per $\alpha\beta$ unit (Seravalli *et al.*, 2003). This correlation relied on the assumption of uniform occupancy of Fe and Ni in the other metal sites in this protein, with 17 metal sites per $\alpha\beta$ unit. However, a negative correlation was found when using a larger number of samples with a larger range in metal occupancy: 1.6–2.8 Ni per $\alpha\beta$ and 0.2–1.1 Cu per $\alpha\beta$ (Seravalli *et al.*, 2004). Furthermore, a positive correlation with Ni (including a slope of 0.5 for the NiFeC signal intensity *versus* Ni, indicating both Ni_p and Ni_d are required) and a negative correlation with Cu strongly indicaties that the CuNi enzyme is inactive and the NiNi is active (Seravalli *et al.*, 2004). Similar results were recently published from the Meyer and Huber groups (Svetlitchnyi *et al.*, 2004). Furthermore, a protocol to generate nearly homogeneous preparations of ACS with a NiFeC signal intensity of ~0.8 spins per mol was achieved by removing Cu with o-phenanthroline and replacing the Cu with Ni (Seravalli *et al.*, 2004). In addition, only Ni, not Cu^{1+} (which was shown by XAS studies to bind to the M_p site), restores activity in o-phenanthroline–treated ACS.

Recent DFT calculations (described below) also indicate that a paramagnetic state of the A-Cluster, called the *NiFeC species*, could derive from the NiNi, but not the CuNi form of the enzyme (Schenker & Brunold, 2003). Multifrequency EPR studies also are inconsistent with the NiFeC EPR signal arising from the CuNi enzyme (Seravalli *et al.*, 2004).

To summarize, it now seems clear that the NiNi form of ACS is active and that the CuNi and the ZnNi forms are not. The apparent vulnerability of the proximal metal site in the A-Cluster to substitution with different metals appears to underlie the heterogeneity observed in samples that has confounded studies of CODH/ACS for many years. Development of a method to replace zinc with Ni would likely produce absolutely homogeneous and fully active ACS.

The FeS cluster component of the A-Cluster is coordinated by four Cys residues, Cys506, Cys509, Cys518, and Cys528, resembling typical [4Fe-4S] clusters found in clostridial ferredoxins, in agreement with EPR (Ragsdale *et al.*, 1985), Mössbauer (Lindahl *et al.*, 1990b; Russell *et al.*, 1998), and ENDOR (Fan *et al.*, 1991) spectroscopic data. Cys509 bridges the [4Fe-4S] cluster and the binuclear site, similar to the Fe-only hydrogenases in which a [4Fe-4S] and a binuclear Fe site are bridged by a Cys residue (Nicolet *et al.*, 2000; Peters *et al.*, 1998). The proximal Ni, *i.e.*, the one closest to the [4Fe-4S] cluster, is coordinated by Cys595, Cys597, and the bridging Cys509. The distal Ni atom has square planar geometry and is coordinated by the sidechains of Cys595 and Cys597 and by two backbone N atoms of Gly596 and Cys597. In one ACS structure, Cu was in high occupancy, forming a binuclear CuNi center (Doukov *et al.*, 2002). In another structure of the same enzyme from the same source (*M. thermoacetica*) containing two ACS molecules in the asymmetric unit, Ni replaced Cu in one A-Cluster (the NiNi enzyme) and Zn was present in the other (ZnNi) (Darnault *et al.*, 2003).

The binuclear nickel active site of the heterologously expressed methanogenic ACS (ACDS, the beta subunit of the five-subunit complex) was studied by XAS and X-ray MCD (Funk *et al.*, 2004; Gu *et al.*, 2003). Two distinct Ni environments were observed: one Ni appears to be square planar, presumably Ni_d, and the other tetrahedral or distorted tetrahedral (apparently Ni_p), which is consistent with the crystal structures. In the as-isolated enzyme, planar Ni_d is low spin and Ni_p is high spin. Reduction with Ti^{3+}-citrate or CO in the presence of Ti^{3+}-citrate appears to reduce some of the Ni_p from Ni^{2+} to Ni^{1+} and a portion of the [4Fe-4S] cluster from the 2+ to the all-ferrous 0+ state. In the CO/Ti^{3+}-treated sample, the tetrahedral high-spin Ni^{2+} (Ni_p) appeared to convert to low-spin Ni^{2+} (Funk *et al.*, 2004), and a feature developed at 2.7 Å that was assigned to a Ni–Fe interaction (Gu *et al.*, 2003). Under all redox conditions, a 2.95 Å vector, assigned to a Ni–Ni interaction was observed. The X-ray absorption near edge spectroscopy (XANES) spectra appear to be inconsistent, with a proposed Ni^0 formulation in any of the states studied. Since the XAS and X-ray MCD studies did not find evidence for significant amounts of Ni^{1+} in the CO-treated sample, it was concluded that reduction of the A-Cluster to form the NiFeC species localizes the radical primarily at a site other than Ni. However, recent computational and spectroscopic studies, described below, indicate that the NiFeC species contains Ni^{1+}-CO (Schenker & Brunold, 2003; Seravalli *et al.*, 2004).

What is the electronic state of the active form of the NiNi enzyme, which is responsible for an EPR signal called the NiFeC signal? Recent Density Functional Theory (DFT) calculations support a model that includes a $[4Fe\text{-}4S]^{2+}$ cluster linked to Ni^{1+} at the M_p site, which is bridged to a Ni^{2+} at the M_d site (Schenker & Brunold, 2003). In this model, the spin resides predominantly on the Ni^{1+}, which has an electronic spin, $S = 1/2$, since the other components of the A-Cluster have net spins, $S = 0$. The NiFeC-eliciting species is described as a $[4Fe\text{-}4S]^{2+}$ (net $S = 0$) cluster bridged to a Ni^{1+} ($S = 1/2$) at M_p that is bridged to square planar Ni^{2+} ($S = 0$) at M_d, with the spin predominantly on the Ni^{1+}. The carbonyl group of the NiFeC species also has spin density based on the observation of ^{13}CO hyperfine splittings (Ragsdale *et al.*, 1983b, 1985). A bridging carbonyl would be a mechanistically interesting possibility; however, the high C–O vibrational frequency (1996 cm^{-1}) clearly indicates a terminal CO bound to one metal (Chen *et al.*, 2003; Kumar & Ragsdale, 1992).

Catalysis: The Condenser of the CODH/ACS Machine. ACS catalyzes the final steps of the Wood-Ljungdahl pathway in which a methyl group, CO, and CoA are condensed to form acetyl-CoA at the A-Cluster of ACS (Figure 15) (also see Fontecilla-Camps and Ragsdale, 1999; Seravalli *et al.*, 1999). In the mechanistically related Monsanto industrial process, a rhodium complex catalyzes acetate formation from methanol and CO in the presence of HI through methyl-Rh, Rh–CO, and acetyl-Rh organometallic intermediates. There are three major controversial issues in the ACS catalytic mechanism: (1) whether the catalytic cycle occurs through diamagnetic or paramagnetic intermediates (in Figure15, both the paramagnetic and diamagnetic mechanisms are presented); (2) whether the central nucleophilic species is a Ni^0, Ni^{1+}, or Ni^{2+} species; and (3) whether the first step in acetyl-CoA synthesis is carbonylation or methylation (here I have presented carbonylation as the first step in both mechanisms). These issues are addressed in a series of articles recently published in the *Journal for Biological Inorganic Chemistry* (Brunold, 2004; Drennan *et al.*, 2004; Lindahl, 2004; Vobeda & Fontecilla-Camps, 2004).

As shown in Figure 15, a channel directs CO to the Ni_p site of the A-Cluster of ACS (Doukov *et al.*, 2002). CO is shown as the first substrate to bind to Ni. In the paramagnetic mechanism (upper figure), the NiFeC species (above) is formed as the central intermediate. This metal-CO complex has been observed by IR (Chen *et al.*, 2003; Kumar & Ragsdale, 1992) and EPR (Ragsdale *et al.*, 1985) spectroscopy (as the NiFeC species) (Figure 16). The NiFeC EPR signal has g values at 2.08 and 2.02, and exhibits ^{61}Ni, ^{13}C, and ^{57}Fe hyperfine interactions (Fan *et al.*, 1991; Ragsdale *et al.*, 1985). The NiFeC species has been demonstrated to be a catalytically competent intermediate in acetyl-CoA synthesis (Seravalli *et al.*, 2002); in the upper mechanism this paramagnetic Ni^{1+}-CO intermediate is the species that undergoes methylation. One complication of the paramagnetic mechanism is that methylation of ACS clearly generates a diamagnetic product (Barondeau &

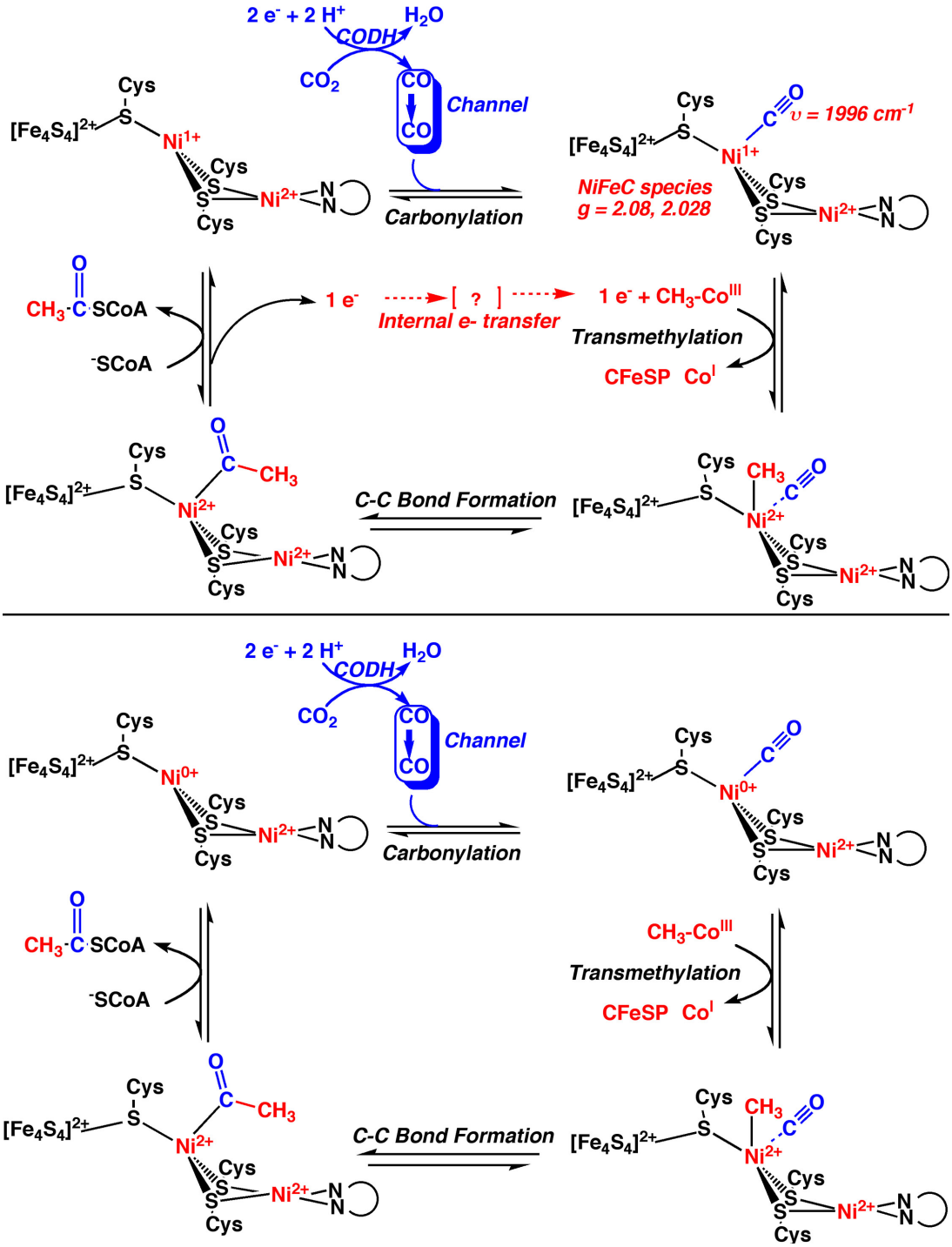

FIG. 15. Two proposed ACS mechanisms. Steps leading to the carbonyl group of acetyl-CoA are shown in blue, while steps involved in forming the methyl group are shown in red. The top figure has been called the paramagnetic mechanism involving the Ni^{1+}-NiFeC species as a central intermediate. The bottom figure is the author's interpretation of a version of the diamagnetic mechanism, which includes a Ni^{0} state as the central intermediate. See the text for details.

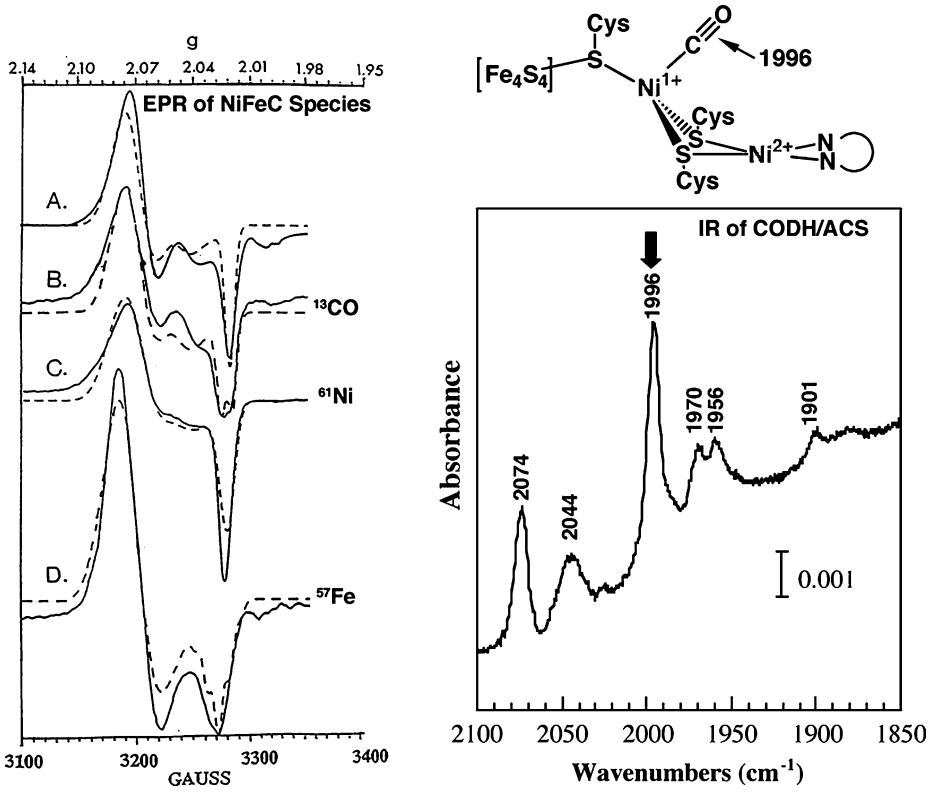

FIG. 16. Spectroscopy of the NiFeC species. Left: EPR spectrum of unlabeled CODH/ACS incubated with natural abundance CO (top) compared with those of enzyme samples labeled with ^{61}Ni or ^{57}Fe or incubated with ^{13} CO (Ragsdale *et al.*, 1985). Right: IR spectra of CODH/ACS after treating with CO. The 1996 cm^{-1} band is from the A-Cluster and the others are from the C-Cluster (modified from Chen *et al.*, 2003).

Lindahl, 1997; Seravalli *et al.*, 2002). Therefore, in the paramagnetic mechanism, an internal electron transfer step is proposed, which prior to, coincident with, or preceding methylation generates methyl-Ni^{2+}. This electron is returned to the donor in the final stages of the catalytic cycle as described below.

The lower scheme in Figure 15 describes a catalytic cycle involving only diamagnetic intermediates (Barondeau & Lindahl, 1997), which involves Ni^0 as the key intermediate (Darnault *et al.*, 2003). In this mechanistic proposal, the paramagnetic NiFeC state is considered to be an inhibited form of the enzyme (Darnault *et al.*, 2003; Tan *et al.*, 2002). The diamagnetic mechanism starts by reductive activation of the enzyme to the Ni^0 state, which undergoes carbonylation to form a Ni^0-CO complex that is methylated by the methylated CFeSP to directly form methyl-Ni^{2+}.

There are chemical precedents supporting both Ni^0 and Ni^{1+} active sites. A model containing a binuclear Ni^0-Ni^{2+}–active site similar to that observed in ACS was shown to form a Ni^0-$(CO)_2$ complex (Linck *et al.*, 2003). However Ni^0-carbonyls are well known and are not considered especially reactive. A Ni^{1+}-CO complex with an IR stretch (1995 cm^{-1}) similar to that of the NiFeC species (above, 1996 cm^{-1}) has been recently characterized, (Craft *et al.*, 2003) and, as described below, methylation of a Ni^{1+} complex by a methyl-Co^{3+} complex, similar to the next step in the ACS reaction sequence, has also been characterized (Ram & Riordan, 1995; Ram *et al.*, 1997). Recent density functional calculations support a Ni^0 mechanism with methylation preceding carbonylation (Webster *et al.*, 2004) as well as a Ni^{1+} mechanism with the opposite binding sequence (Schenker & Brunold, 2003).

The next step in the ACS mechanism is methylation of the A-Cluster by the methyl-Co^{3+} form of the CFeSP (Seravalli *et al.*, 2002). Based on rapid kinetic studies, this reaction appears to occur by the S_N2-type nucleophilic attack of Ni_p on the methyl group of the methylated CFeSP (CH_3-Co^{3+}) to generate methyl-Ni and Co^{1+} (Menon & Ragsdale, 1998, 1999). This mechanism is reminiscent of the reactions of cobalamin-dependent methyltransferases like methionine synthase (Banerjee & Ragsdale, 2003; Matthews, 2001) and is supported by stereochemical studies using a chiral methyl donor (Lebertz *et al.*, 1987). This transmethylation reaction is reversible and is linearly dependent on methyl-CFeSP (forward reaction) or CFeSP (back reaction), yielding second-order rate constants of 0.047 μM^{-1} s^{-1} (forward) and 0.4 μM^{-1} s^{-1} (reverse)

with a Keq of 0.12 (Seravalli *et al.*, 2002). In another set of studies, when this reaction was modeled as a three-step process, the methylation rate constant was 12 $\mu M^{-1}s^{-1}$ (forward) and the reverse rate constant was 2 μM^{-1} s^{-1} (Tan *et al.*, 2003). Thus, the Ni^{1+} site on ACS appears to be about as effective as Co^{1+}-CFeSP as a methyl group acceptor. At low CO concentrations, formation of this intermediate is rate limiting in the overall pathway of acetyl-CoA synthesis; however, at higher CO concentrations (which inhibit acetyl-CoA synthesis Maynard *et al.*, 2001), methyl transfer becomes rate limiting (Seravalli *et al.*, 2002). It is the methyl transfer step that is inhibited by CO, perhaps by the binding of a second CO to the site of methylation (Seravalli *et al.*, 2002). What state of ACS is the methyl acceptor? Based on studies of the overall reaction sequence of ACS by rapid kinetics, steady-state kinetic experiments and kinetic simulations (Seravalli *et al.*, 2002), the NiFeC species is kinetically competent in the acetyl-CoA synthesis catalytic cycle.

As described above in the ACS structure section, the recent crystal structures provide strong evidence for major conformational changes during this reaction. There is evidence that the methyl group binds to the labile Ni site of the A-Cluster (Barondeau & Lindahl, 1997; Shin *et al.*, 1993) that, based on XAS studies, appears to be Ni_p (Seravalli *et al.*, 2004). Kinetic and spectroscopic studies indicate that this methyl transfer involves an S_N2 reaction (Menon & Ragsdale, 1999). Interestingly, in model studies of the reaction between methyl-Co^{3+} (CH_3-Co^{3+} dimethylglyoximate) and a Ni^{1+} macrocycle, transfer of a methyl radical is favored over a methyl cation transfer. Two equivalents of the Ni^{1+} complex were required, one to reduce methyl-Co^{3+} to methyl-Co^{2+} and the other to capture the methyl radical generated upon cleavage of the methyl-Co^{2+} species (Ram & Riordan, 1995). Follow-up experiments with these model reactions using radical traps also support a methyl radical transfer reaction (Ram *et al.*, 1997). However, Martin and Finke (1990) pointed out that for the enzymatic system, homolysis of the CH_3-Co bond could not occur because reduction of CH_3-Co^{3+} requires redox potentials (<-1 V) that are too low for physiological electron donors.

The methyl transfer step as shown in Figure 15 includes a one-electron shuttle, *i.e.*, one electron is donated during the methylation and an electron is lost after CoA binds. Inclusion of this redox step in the ACS mechanism would explain why reaction of the NiFeC species with the methylated CFeSP generates a diamagnetic methyl-Ni^{2+} product (Barondeau & Lindahl, 1997; Seravalli *et al.*, 2002). If a methyl-Ni^{3+} were generated, it would be EPR active. Another reason that a methyl-Ni^{3+} species is not favored is that it would be highly oxidizing and quite reactive (Thauer, 1998). One obvious candidate for this one-electron shuttle is the [4Fe-4S] subcomponent of the A-Cluster, which is only a spectator in the two schemes shown in Figure 15. Demonstration that this cluster undergoes reduction at a slower rate than the methyl group is transferred apparently rules out such a role for this cluster (Tan *et al.*, 2003); however, if the methylation and reduction were coupled, the rate of reduction of the cluster could increase significantly. On the other hand, perhaps it serves only as a conduit for electron transfer to the Ni. Lindahl's diamagnetic Ni^0 mechanism avoids the need for redox shuttling because reaction of a methyl cation wih Ni^0 would directly generate a diamagnetic CH_3-Ni^{2+}. The significant stimulation of the CO/acetyl-CoA exchange reaction, which does not involve net redox chemistry, by ferredoxin and other one-electron carriers is considered to support an internal electron transfer reaction during catalysis (Ragsdale & Wood, 1985). The ferredoxin-binding site shown in purple in the CODH/ACS structure is close enough to participate in shuttling (donating and then receiving) one electron during this reaction.

Carbon–carbon bond formation, the next step in the catalytic cycle, occurs by condensation of the methyl and carbonyl groups to form an acetyl-metal species. There is evidence that this intermediate was trapped in crystals of CODH/ACS incubated in a solution containing high concentrations of acetate (Doukov *et al.*, 2002).

The final steps in the catalytic cycle involve binding of CoA and thiolysis of the acetyl-metal bond. CoA appears to ligate to the proximal metal site in the A-Cluster, based on the observation of a Se-Cu bond by EXAFS of the CuNi form of CODH/ACS incubated with seleno-CoA (Seravalli *et al.*, 2003). In the diamagnetic mechanism, the two electrons liberated during the thiolysis are used to reduce the Ni^{2+} back to catalytically active Ni^0. In the paramagnetic mechanism, one electron reduces Ni^{2+} back to Ni^{1+} and the other is returned to the one-electron shuttle.

Thus, the Wood-Ljungdahl pathway appears to represent a prototypical bio-organometallic pathway involving, like the Monsanto process, methyl-metal, metal-CO, and acetyl-metal intermediates. Interestingly, when ACS undergoes reductive activation and binds CoA and the methylated CFeSP, the rate of CO formation by CODH and acetyl-CoA synthesis by ACS become synchronized (Maynard & Lindahl, 2001). The structural transformations accompanying this transformation are not known, but may relate to alterations in function of the CO channel or the rate of the conformational change described above. Uncovering how these active sites are coupled is an exciting area for future research.

Other Wood-Ljungdahl Pathway Enzymes Required for CO Utilization

The focus of this review so far has been on CODH and CODH/ACS since these enzymes are key to CO

metabolism. However, for organisms that use the Wood-Ljungdahl pathway (Figure 1), a number of additional enzymes are required.

Conversion of CO_2 to CH_3-H_4 folate. The methyl or Eastern branch of this pathway (Figure 1) includes five enzymes required for catalyzing the synthesis of the methyl group of CH_3-H_4folate from CO_2 (Ljungdahl, 1986; Ragsdale, 1991). These include formate dehydrogenase, which converts CO_2 to formate (Andreesen *et al.*, 1973; Ljungdahl & Andreesen, 1978). Then, formyl-H_4 folate synthetase catalyzes the ATP-dependent conversion of formate to 10-formyl-H_4folate (Brewer *et al.*, 1970; Lovell *et al.*, 1990; Sun *et al.*, 1969), which is converted by a cyclohydrolase to 5,10-methenyl-H_4folate (Clark & Ljungdahl, 1982). Next, a dehydrogenase reduces methenyl- to 5,10-methylene-H_4folate, (Ljungdahl *et al.*, 1980; Moore *et al.*, 1974; O'Brien *et al.*, 1973; Ragsdale & Ljungdahl, 1984b) which is reduced to CH_3-H_4folate by a reductase (Clark & Ljungdahl, 1984; Park *et al.*, 1991). Since these reactions were reviewed in 1991 (Ragsdale, 1991) and 2003 (Ragsdale, 2003a), it is unnecessary to cover them here. A similar series of reactions is involved in the conversion of formate to methyltetrahydropterin by methanogens and these reactions also were recently reviewed (Ragsdale, 2003a).

Conversion of CH_3-H_4 folate to CH_3-CFeSP. The MeTr-catalyzed transfer of the methyl group of CH_3-H_4 folate to the CFeSP (Figure 17) also has been reviewed recently (Banerjee & Ragsdale, 2003) and will only be briefly covered here. In 1984, Hu *et al.* partially purified a corrinoid-containing protein that accepts the methyl group of CH_3-H_4folate to form methyl-cobamide (Hu *et al.*, 1984). This protein was then purified to homogeneity and, because it was shown to contain an iron-sulfur cluster, was named the *corrinoid iron-sulfur protein* (CFeSP) (Ragsdale *et al.*, 1987). The CFeSP accepts the N^5 methyl group of CH_3-H_4folate in a reaction catalyzed by methyltransferase (MeTr) (Drake *et al.*, 1981) and then transfers this methyl group to the A-Cluster on demethylated CODH/ACS (above). This reaction initiates the carbonyl or Western branch of the acetyl-CoA pathway. MeTr has been purified to homogeneity (Drake *et al.*, 1981), and its structure was determined by X-ray crystallography (Doukov *et al.*, 2000), demonstrating that it belongs to the class of "TIM-barrel" proteins. The MeTr gene has been cloned, sequenced, and overexpressed in an active form in *E coli* (Roberts *et al.*, 1989, 1994).

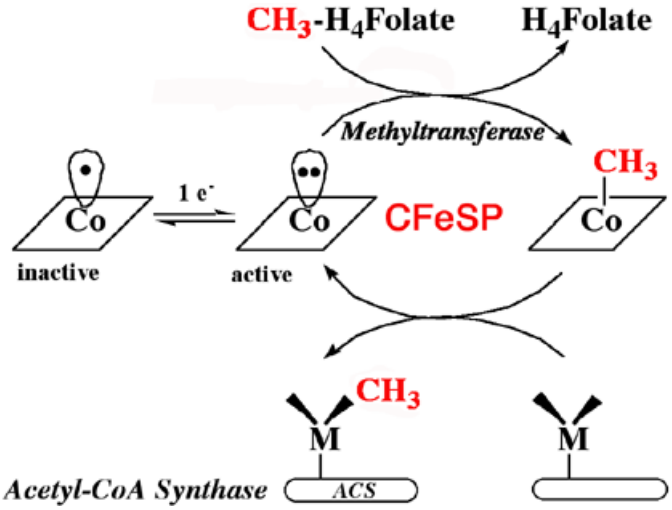

FIG. 17. Methyl transfer to form the first organometallic intermediate in the Wood-Ljungdahl pathway. The Co^{1+} state of the CFeSP, which is the active state, is in redox equilibrium with Co^{2+}, which requires reductive activation to reenter the catalytic cycle.

Although MeTr can use either vitamin B_{12} or the CFeSP as the methyl acceptor, its specificity (k_{cat}/K_m) for the CFeSP is 100-fold greater than that for free B_{12} (Zhao *et al.*, 1995). The steps in the MeTr mechanism include: (1) a pH-dependent conformational change in MeTr (Zhao & Ragsdale, 1996), (2) CH_3-H_4folate and the CFeSP binding to MeTr in a rapid equilibrium fashion to form a ternary complex, (3) protonation of the N-5 of CH_3-H_4 folate, (4) methyl transfer from CH_3-N of the pterin to Co^{1+} to form H_4folate and CH_3-CFeSP, and (5) products dissociation (Seravalli *et al.*, 1999). The protonation step is required for electrophilic activation of the methyl group, making it more susceptible to nucleophilic displacement by the cob(I)amide state of the CFeSP.

Besides electrophilic activation of CH_3-H_4folate, this reaction also requires reductive activation of the CFeSP. This is because the transmethylation reaction requires the Co^{1+} state, and once in every 100 turnovers the cobalt center undergoes oxidation to the inactive Co^{2+} state (Menon & Ragsdale, 1999). The low potential [4Fe-4S] cluster is required to mediate electron transfer from physiological electron donors to the cobalt center (Menon & Ragsdale, 1998), which regenerates the active Co^{1+} state. The CFeSPs of acetogens and methanogens are unusual in that they lack either an intramolecular benzimidazole base or a histidine residue (that ligates to Co in many B_{12} proteins) (Ragsdale *et al.*, 1987; Wirt *et al.*, 1993, 1995). The absence of this ligand makes the Co-bound methyl group more susceptible to nucleophilic attack and increases the midpoint potential of the $Co^{2+/1+}$ couple by about 150 mV, which would allow the cell to maintain more Co in the active Co^{1+} state (Harder *et al.*, 1989). Thus, controlling cobalt coordination chemistry prevents Co^{1+} from dropping out of the catalytic cycle.

Conversion of Acetyl-CoA to Pyruvate. PFOR catalyzes the thiamine pyrophosphate (TPP)-dependent oxidative decarboxylation of pyruvate to form acetyl-CoA and CO_2 (Equation (7)). A detailed review of PFOR was published this year, so this section will be brief (Ragsdale, 2003b). All members of the Archaea kingdom appear to contain PFOR, and it is widely distributed among anaerobic bacteria and anarobic protozoa like Giardia
(Horner *et al.*, 1999). PFORs has been isolated from the acetogenic bacterium *Moorella thermoacetica* (f. *Clostridium thermoaceticum*) (Drake *et al.*, 1981; Menon & Ragsdale, 1996a) and other Clostridia, (Uyeda & Rabinowitz, 1971) from the methanogenic archaea,-*Methanosarcina barkeri* (Bock *et al.*, 1994) and *Methanobacterium thermoautotrophicum* (Tersteegen *et al.*, 1997), and from several hyperthermophilic archaea (Adams & Kletzin, 1996).

The oxidation of pyruvate by PFOR generates low potential electrons ($Eo' = -540$ mV) that reduce ferredoxin or flavodoxin (Brostedt & Nordlund, 1991; Cammack *et al.*, 1980; Hughes *et al.*, 1995; Kerscher & Oesterhelt, 1982; Kletzin & Adams, 1996; Wahl & Orme-Johnson, 1987). This reaction occurs extremely rapidly, with a second order rate constant of 2–7 $\times$ 10^7 $M^{-1}s^{-1}$ for the *D. africanus* (Pieulle *et al.*, 1999) and the *M. thermoacetica* (Furdui & Ragsdale, 2002) PFORs. Since the PFOR reaction is reversible, the enzyme has also been called pyruvate synthase. In methanogens and other anaerobic microbes synthesizing cell carbon by the Wood-Ljungdahl pathway, pyruvate formation is a most important reaction because it links the Wood-Ljungdahl pathway to the incomplete reductive tricarboxylic acid cycle, which generates biosynthetic intermediates. The tremendous energy barrier for pyruvate formation appears to be accomplished by reverse electron transfer involving coupling of H_2 oxidation by the membrane-associated *Ech* hydrogenase to the membrane (Meuer *et al.*, 2002). Two genes were recently discovered that encode proteins (PorE and PorF) and are components of a specialized system required to transfer low-potential electrons for pyruvate biosynthesis (Lin & Whitman, 2003; Lin *et al.*, 2003).

PFOR(EC1.2.7.1):

$$\text{pyruvate} + \text{CoA} + 2\text{Fd(ox)} \rightarrow \text{CO}_2 + \text{H}^+ + \text{acetyl-CoA} + 2\text{Fd(red)} \qquad [7]$$

The crystal structure of the *Desulfovibrio africanus* PFOR was determined (Chabriere *et al.*, 1999). This protein contains 7 structural domains. The active site contains TPP and a proximal $[4Fe\text{-}4S]^{2+/1+}$ cluster, which are buried within the protein. Two additional $[4Fe\text{-}4S]^{2+/1+}$ clusters lead to the surface, where interactions with a redox partner such as ferredoxin can occur (Chabriere *et al.*, 1999). Each of the three clusters is separated by ~13 Å (center-to-center).

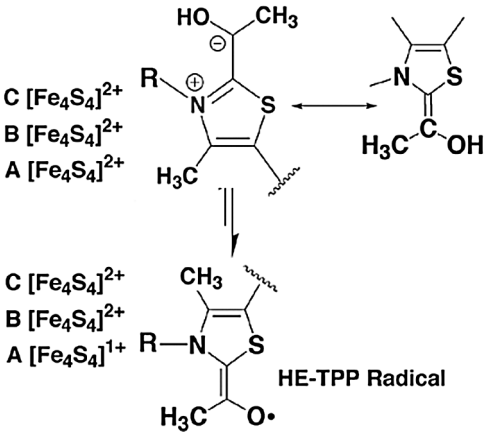

FIG. 18. Formation of the substrate-derived HE-TPP radical intermediate. Electron transfer from HE-TPP to an FeS cluster results in formation of the HE-TPP radical and reduction of a [4Fe-4S] Cluster. The radical is shown as a pi radical, which is consistent with recent spectroscopic studies of PFOR.

Two key steps in the mechanism are the generation and decay of a substrate-derived hydroxyethyl-TPP radical (HE-TPP) intermediate (Figure 18). The radical intermediate has been captured at 80% occupancy in the crystal structure of the PFOR from *D. africanus* (Chabriere *et al.*, 2001). A provocative hypothesis proposed that the thiazolium ring has lost its aromaticity in the radical intermediate to form a σ/n-type radical. Unusual characteristics of this radical are ketonization of the hydroxy group at C2α to form an acetyl radical, a long C2-C2α bond, sp^3 hybridization at thiazolium atoms N3 and C5, and tautomerization of the C4-C5 double bond to give an exocyclic double bond. This proposed structure requires further validation to ensure that it is consistent with EPR spectroscopic data, since some preliminary results indicate that the radical may be best explained as a π radical. The figure shows the radical localized on oxygen, but since the thiazolium is aromatic, the spin density would be somewhat delocalized over the thiazolium ring.

When the rate constants for the different steps in the PFOR mechanism were determined, it was found that CoA increases the rate of electron transfer from the radical to one of the [4Fe-4S] clusters in the protein by 10^5–fold (Furdui & Ragsdale, 2002; Menon & Ragsdale, 1997). Analysis by Marcus theory indicates the thiol group of CoA lends over 40 kJ/mol to the electron transfer rate enhancement (Furdui & Ragsdale, 2002). Future experiments will be aimed at elucidating how CoA increases the rate of this electron transfer reaction.

PERSPECTIVES

This review has focused on the biochemistry of microbial carbon monoxide metabolism. It now appears plausible that the use of CO is an evolutionarily ancient process, perhaps initiating with simple metal clusters and increasing in efficiency as the metallocenters became enveloped by peptides and then by complex evolving proteins. The structures of three distinct types of proteins that metabolize CO have appeared, along with one that controls gene expression in response to the presence of CO. In sum, four different transition metals (Cu, Ni, Fe, and Mo) in different arrangements are the cornerstones of CO metabolism.

Mutagenesis and spectroscopic studies are uncovering how ligand exchange reactions, apparently coupled to conformational changes in a long helix at the subunit interface, control whether the heme-based CO sensor binds DNA or not. A crystal structure of the CO-bound form of this protein will be important in further understanding this system.

A Cu molybdopterin center that has relatively low efficiency has been shown to be responsible for CO oxidation in some aerobic bacteria, while Ni-Fe-S centers prevail in the anaerobic world. Remarkably, two different Ni metallocenters in apparently unrelated proteins have evolved: a $NiFe_4S_4$ center in CODH to oxidize CO at rates exceeding 10^9 $M^{-1}s^{-1}$ and a $Ni_2Fe_4S_4$ center in ACS to synthesize the key metabolic building block acetyl-CoA by condensing CO with a methyl group and Coenzyme A. The long-awaited molecular structures of these catalysts are now known. Now biological, computational, synthetic, structural, and physical chemists are at this scientific frontier attempting to understand how these remarkable bioorganometallic reactions occur. Over the next few years, we can hope that the crystal structures of the intermediates can be determined, including M-CO, M-CH_3, M-acetyl, M-SCoA for ACS and M-CO, M-hydroxide, perhaps even M-CO_2 for CODH. One can also expect to learn more about how conformational changes in the CODH/ACS are coordinated with catalysis. Hopefully, questions about whether the catalytic cycles operate through paramagnetic or diamagnetic mechanisms will be clearly resolved by scientists who are at work modeling, calculating, modifying, measuring, and visualizing the enzymes and their active centers.

One of the most exciting recent findings has been the discovery of a long channel that directs CO that is generated by CODH to the ACS active site. The chemical nature of this channel will soon be revealed and we will have a better understanding of how one can direct the movement of a small hydrophobic gas molecule over relatively long distances. Precise functioning of this channel is paramount to the proper operation of the CODH/ACS nanomachine.

CO metabolism is linked to pathways for energy generation and cell carbon synthesis in these organisms. We will soon see the crystal structure of MeTr with bound CH_3-H_4folate, which will help us understand the nature of electrophilic activation of the methyl group. How the pterin and the Co center, bound to the CFeSP, are positioned in the transition state, and how protonation of the pterin is linked to methyl transfer, will continue to be the focus of studies on this class of proteins.

The crystal structure of PFOR, which links CO metabolism to cell carbon synthesis, has appeared. This is an entirely different mechanism of acetyl-CoA synthesis. We will soon have a revised structure of the substrate-derived HE-TPP radical intermediate in the PFOR mechanism. Over the next few years, the reader can expect to learn how this radical reacts with the thiol of CoA to generate acetyl-CoA. Generation of pyruvate from acetyl-CoA is a Herculean task, and how energy is transformed to accomplish this uphill reaction will be an exciting area.

It seems a safe bet that studies of CO metabolism will continue to be an exciting research area for microbiologists, biochemists, chemists, and physicists. This research is also expected to be an area for chemical and biological engineers to develop new catalysts that can help solve some environmental problems, like lowering greenhouse gas levels and cleaning up hazardous wastes, and facilitate difficult chemistry, like CO_2 activation.

ACKNOWLEDGEMENTS

I thank Gary Roberts and David Grahame for their useful comments and suggestions on the manuscript. I thank my students and postdoctors for their dedicated work on the CODH/ACS system, especially Javier Seravalli who has worked on all of the Wood-Ljungdahl pathway proteins. I am grateful to Lars Ljungdahl for introducing me to acetogenic bacteria as a graduate student at Georgia and the late Harland Wood for supporting my work on this system as a postdoctor at Case Western Reserve University. I am greatly appreciative of various collaborators who have worked with me on different aspects of the Wood-Ljungdahl pathway, especially Bill Antholine, Kim Bagley, Tadhg Begley, Thomas Brunold, Steve Cramer, Tzanko Doukov, Cathy Drennan, Juan Fontecilla-Camps, Gary Gerfen, Weiwei Gu, and Tom Spiro over the last few years.

REFERENCES

Adams, M.W.W. and Kletzin, A. 1996. Oxidoreductase-type enzymes and redox proteins involved in fermentative metabolisms of hyperthermophilic archaea. *Adv Protein Chem* **48:**101–180.

Anderson, M.E., DeRose, V.J., Hoffman, B.M., and Lindahl, P.A. 1993. Identification of a cyanide binding site in CO dehydrogenase from *Clostridium thermoaceticum* using EPR and ENDOR spectroscopies. *J Am Chem Soc* **115:**12204–12205.

Andreesen, J.R., Schaupp, A., Neurater, C., Brown, A., and Ljungdahl, L.G. 1973. Fermentation of glucose, fructose, and xylose by *Clostridium thermoaceticum*: effect of metals on growth yield, enzymes, and the synthesis of acetate from CO_2. *J Bacteriol* **114:**743–751.

Aono, S. 2003. Biochemical and biophysical properties of the CO-sensing transcriptional activator CooA. *Acc Chem Res* **36:**825–831.

Aono, S., Nakajima, H., Saito, K., and Okada, M. 1996. A novel heme protein that acts as a carbon monoxide- dependent transcriptional activator in Rhodospirillum rubrum. *Biochem Biophys Res Commun* **228**(3):752–756.

Arendsen, A.F., Soliman, M.Q., and Ragsdale, S.W. 1999. Nitrate-dependent regulation of acetate biosynthesis and nitrate respiration by Clostridium thermoaceticum. *J Bacteriol* **181**(5):1489–1495.

Bagley, K.A., Duin, E.C., Roseboom, W., Albracht, S.P.J., and Woodruff, W.H. 1995. Infrared-detectable groups sense changes in charge density on the nickel center in hydrogenase from *Chromatium vinosum*. *Biochemistry* **34**(16):5527–5535.

Banerjee, R. and Ragsdale, S.W. 2003. The many faces of vitamin B_{12}: Catalysis by cobalamin-dependent enzymes. *Ann Rev Biochem* **72:**209–247.

Barondeau, D.P. and Lindahl, P.A. 1997. Methylation of carbon monoxide dehydrogenase from Clostridium thermoaceticum and mechanism of acetyl coenzyme A synthesis. *J Am Chem Soc* **119**(17):3959–3970.

Bartholomew, G.W. and Alexander, M. 1979. Microbial metabolism of carbon monoxide in culture and in soil. *Appl Environ Microbiol* **37:**932–937.

Beijerinck, M. and van Delden, A. 1903. On a colorless bacterium, whose carbon-food comes from the atmosphere. *Proc Section Sci Kon Akademie van Wetenschappen, Amsterdam*, **5:**389–413.

Bertini, I. and Luchinat, C. 1994. The reaction pathways of zinc enzymes and related biological catalysts. In: *Bioinorganic chemistry*, pp. 31–106. I. Bertini, H.B. Gray, S.J. Lippard, and J.S. Valentine, Eds., University Science Books, Mill Valley, CA.

Bhatnagar, L., Krzycki, J.A., and Zeikus, J.G. 1987. Analysis of hydrogen metabolism in Methanosarcina barkeri: regulation of hydrogenase and role of CO-dehydrogenase in H_2 production. *FEMS Microbiol Lett* **41:**337–343.

Black, G.W., Lyons, C.M., Williams, E., Colby, J., Kehoe, M., and O'Reilly, C. 1990. Cloning and expression of the carbon monoxide dehydrogenase genes from *Pseudomonas thermocarboxydovorans* strain C2. *FEMS Microbiol Lett* **58:**249–254.

Bock, A.-K., Prieger-Kraft, A., and Schönheit, P. 1994. Pyruvate—a novel substrate for growth and methane mormation in *Methanosarcina barkeri*. *Arch Microbiol* **161:**33–46.

Boehning, D. and Snyder, S.H. 2003. Novel neural modulators. *Annu Rev Neurosci* **26:**105–131.

Bramlett, M.R., Tan, X., and Lindahl, P.A. 2003. Inactivation of acetyl-CoA synthase/carbon monoxide dehydrogenase by copper. *J Am Chem Soc* **125**(31):9316–9317.

Bray, R.C., George, G.N., Lange, R., and Meyer, O. 1983. Studies by e.p.r. spectroscopy of carbon monoxide oxidases from *Pseudomonas carboxydovorans* and *Pseudomonas carboxydohydrogena*. *Biochem J.* **211:**687–694.

Brewer, J.M., Ljungdahl, L., Spencer, T.E., and Neece, S.H. 1970. Physical properties of formyltetrahydrofolate synthetase from *Clostridium thermoaceticum*. *J Biol Chem* **245**(18):4798–4803.

Brock, T. and Schlegel, H. 1989. Introduction. In *Autotrophic bacteria*, pp. 1–15. H. Schlegel and B. Bowien, Eds., Science Tech Publishers, Madison, WI.

Brock, T.D. 1989. Evolutionary relationships of the autotrophic bacteria. In *Autotrophic bacteria*, pp. 499–512. H.G. Schlegel and B. Bowien, Eds., Science Tech Publishers, Madison, WI.

Brostedt, E. and Nordlund, S. 1991. Purification and partial characterization of a pyruvate oxidoreductase from the photosynthetic bacterium Rhodospirillum rubrum grown under nitrogen-fixing conditions. *Biochem J* **279**(Pt 1):155–158.

Brunold, T.C. 2004. Spectroscopic and computational insights into the geometric and electronic properties of the A cluster of acetyl-coenzyme A synthase. *J Biol Inorg Chem* in press.

Cammack, R., Kerscher, I., and Oesterhelt, D. 1980. A stable free radical intermediate in the reaction of 2-oxoacid: ferredoxin oxidoreductases of Halobacterium halobium. *FEBS Lett* **118:**271–273.

Chabriere, E., Charon, M.-H., Volbeda, A., Pieulle, L., Hatchikian, E.C., and Fontecilla-Camps, J.-C. 1999. Crystal structures of the key anaerobic enzyme pyruvate: ferredoxin oxidoreductase, free and in complex with pyruvate. *Nat Struct Biol* **6**(2):182–190.

Chabriere, E., Vernede, X., Guigliarelli, B., Charon, M.H., Hatchikian, E.C., and Fontecilla-Camps, J.C. 2001. Crystal structure of the free radical intermediate of pyruvate:ferredoxin oxidoreductase. *Science* **294**(5551):2559–2563.

Cheesbrough, T.M. and Kolattukudy, P.E. 1984. Alkane biosynthesis by decarbonylation of aldehydes catalyzed by a particulate preparation from Pisum sativum. *Proc Nat Acad Sci USA* **81:**6613–6617.

Chen, J., Huang, S., Seravalli, J., Jr., H.G., Swartz, D.J., Ragsdale, S.W., and Bagley, K.A. 2003. Infrared studies of carbon monoxide binding to carbon monoxide dehydrogenase/acetyl-CoA synthase from *Moorella thermoacetica*. *Biochemistry* **42**(50):14822–14830.

Chen, Z., Lemon, B.J., Huang, S., Swartz, D.J., Peters, J.W., and Bagley, K.A. 2002. Infrared studies of the CO-inhibited form of the Fe-only hydrogenase from Clostridium pasteurianum I: examination of its light sensitivity at cryogenic temperatures. *Biochemistry* **41**(6):2036–2043.

Clark, J.E. and Ljungdahl, L.G. 1982. Purification and properties of 5,10-methenyltetrahydrofolate cyclohydrolase. *J Biol Chem* **257:**3833–3836.

Clark, J.E. and Ljungdahl, L.G. 1984. Purification and properties of 5,10-methylenetetrahydrofolate reductase, an iron-sulfur flavoprotein from Clostridium formicoaceticum. *J Biol Chem* **259:**10845–10889.

Coyle, C.M., Puranik, M., Youn, H., Nielsen, S.B., Williams, R.D., Kerby, R.L., Roberts, G.P., and Spiro, T.G. 2003. Activation mechanism of the CO sensor CooA. Mutational and resonance Raman spectroscopic studies. *J Biol Chem* **278**(37):35384–35393.

Crabtree, R.H. 1988. *The organometallic chem of the transition metals*, John Wiley, New York.

Craft, J.L., Mandimutsira, B.S., Fujita, K., Riordan, C.G., and Brunold, T.C. 2003. Spectroscopic and computational studies of a Ni(+)-CO model complex: implications for the acetyl-CoA synthase catalytic mechanism. *Inorg Chem* **42**(3):859–867.

Dai, Y., Wensink, P.C., and Abeles, R.H. 1999. One protein, two enzymes. *J Biol Chem* **274**(3):1193–1195.

Daniel, S.L., Hsu, T., Dean, S.I., and Drake, H.L. 1990. Characterization of the H_2- and CO-dependent chemolithotrophic potentials of

the acetogens *Clostridium thermoaceticum* and *Acetogenium kivui*. *J Bacteriol* **172:**4464–4471.

Darnault, C., Volbeda, A., Kim, E.J., Legrand, P., Vernede, X., Lindahl, P.A., and Fontecilla-Camps, J.C. 2003. Ni-Zn-[Fe(4)-S(4)] and Ni-Ni-[Fe(4)-S(4)] clusters in closed and open alpha subunits of acetyl-CoA synthase/carbon monoxide dehydrogenase. *Nat Struct Biol* **10**(4):271–279.

DeRose, V.J., Telser, J., Anderson, M.E., Lindahl, P.A., and Hoffman, B.M. 1998. A multinuclear ENDOR study of the C-cluster in CO dehydrogenase from Clostridium thermoaceticum: evidence for HxO and histidine coordination to the [Fe4S4] center. *J Am Chem Soc* **120**(34):8767–8776.

Diekert, G., Hansch, M., and Conrad, R. 1984. Acetate synthesis from 2 CO_2 in acetogenic bacteria: is carbon monoxide an intermediate? *Arch Microbiol* **138:**224–228.

Diekert, G. and Ritter, M. 1983. Purification of the nickel protein carbon monoxide dehydrogenase of *Clostridium thermoaceticum*. *FEBS Lett* **151:**41–44.

Diekert, G. and Thauer, R.K. 1980. The effect of nickel on carbon monoxide dehydrogenase formation in *Clostridium thermoaceticum* and *Clostridium formicoaceticum*. *FEMS Microbiol Lett* **7:**187–189.

Diekert, G.B., Graf, E.G., and Thauer, R.K. 1979. Nickel requirement for carbon monoxide dehydrogenase formation in *Clostridium thermoaceticum*. *Arch Microbiol* **122:**117–120.

Diekert, G.B. and Thauer, R.K. 1978. Carbon monoxide oxidation by *Clostridium thermoaceticum* and *Clostridium formicoaceticum*. *J Bacteriol* **136:**597–606.

Dioum, E.M., Rutter, J., Tuckerman, J.R., Gonzalez, G., Gilles-Gonzalez, M.A., and McKnight, S.L. 2002. NPAS2: a gas-responsive transcription factor. *Science* **298**(5602):2385–2387.

Dobbek, H., Gremer, L., Kiefersauer, R., Huber, R., and Meyer, O. 2002. Catalysis at a dinuclear [CuSMo(==O)OH] cluster in a CO dehydrogenase resolved at 1.1-A resolution. *Proc Natl Acad Sci USA* **99**(25):15971–15976.

Dobbek, H., Gremer, L., Meyer, O., and Huber, R. 1999. Crystal structure and mechanism of CO dehydrogenase, a molybdo iron-sulfur flavoprotein containing S-selanylcysteine. *Proc Natl Acad Sci USA* **96**(16):8884–8889.

Dobbek, H., Svetlitchnyi, V., Gremer, L., Huber, R., and Meyer, O. 2001. Crystal structure of a carbon monoxide dehydrogenase reveals a [Ni-4Fe-5S] cluster. *Science* **293**(5533):1281–1285.

Dore, J., Morvan, B., Rieu-Lesme, F., Goderel, I., Gouet, P., and Pochart, P. 1995. Most probable number enumeration of H2-utilizing acetogenic bacteria from the digestive tract of animals and man. *FEMS Microbiol Lett* **130**(1):7–12.

Doukov, T., Seravalli, J., Stezowski, J., and Ragsdale, S.W. 2000. Crystal structure of a methyltetrahydrofolate and corrinoid dependent methyltransferase. *Structure* **8:**817–830.

Doukov, T.I., Iverson, T., Seravalli, J., Ragsdale, S.W., and Drennan, C.L. 2002. A Ni-Fe-Cu center in a bifunctional carbon monoxide dehydrogenase/acetyl-CoA synthase. *Science* **298**(5593):567–572.

Drake, H.L., Hu, S.-I., and Wood, H.G. 1980. Purification of carbon monoxide dehydrogenase, a nickel enzyme from *Clostridium thermoaceticum*. *J Biol Chem* **255:**7174–7180.

Drake, H.L., Hu, S.-I., and Wood, H.G. 1981. Purification of five components from *Clostridium thermoacticum* which catalyze synthesis of acetate from pyruvate and methyltetrahydrofolate. Properties of phosphotransacetylase. *J Biol Chem* **256:**11137–11144.

Drennan, C.L., Doukov, T.I., and Ragsdale, S.W. 2004. The metallo-clusters of carbon monoxide dehydrogenase/acetyl-CoA synthase: A story in pictures. *J Biol Inorg Chem* in press.

Drennan, C.L., Heo, J., Sintchak, M.D., Schreiter, E., and Ludden, P.W. 2001. Life on carbon monoxide: X-ray structure of Rhodospirillum rubrum Ni-Fe-S carbon monoxide dehydrogenase. *Proc Natl Acad Sci USA* **98**(21):11973–11978.

Ensign, S.A., Bonam, D., and Ludden, P.W. 1989. Nickel is required for the transfer of electrons from carbon monoxide to the iron-sulfur center(s) of carbon monoxide dehydrogenase from Rhodospirillum rubrum. *Biochem* **28**(12):4968–4973.

Fan, C., Gorst, C.M., Ragsdale, S.W., and Hoffman, B.M. 1991. Characterization of the Ni-Fe-C complex formed by reaction of carbon monoxide with the carbon monoxide dehydrogenase from *Clostridium thermoaceticum* by Q-band ENDOR. *Biochemistry* **30:**431–435.

Feng, J. and Lindahl, P.A. 2004. Carbon monoxide dehydrogenase from Rhodospirillum rubrum: effect of redox potential on catalysis. *Biochemistry* **43**(6):1552–1559.

Fontecilla-Camps, J.-C., and Ragsdale, S.W. 1999. Nickel-iron-sulfur active sites: hydrogenase and CO dehydrogenase. In *Advances in Inorganic Chemistry*, Vol. 47, pp. 283–333. A.G. Sykes and R. Cammack, Eds., Academic Press, Inc., San Diego, CA.

Ford, P.A. and Rokicki, A. 1988. Nucleophilic activation of carbon monoxide. Applications to homogeneous catalysis by metal carbonyls. *Adv Organometal Chem* **28:**139–218.

Fox, J.D., He, Y.P., Shelver, D., Roberts, G.P., and Ludden, P.W. 1996. Characterization of the region encoding the CO-induced hydrogenase of Rhodospirillum rubrum. *J Bacteriol* **178**(21):6200–6208.

Funk, T., Gu, W., Friedrich, S., Wang, H., Gencic, S., Grahame, D.A., and Cramer, S.P. 2004. Chemically distinct Ni sites in the A-cluster in subunit beta of the acetyl-CoA decarbonylase/synthase complex from Methanosarcina thermophila: Ni L-edge absorption and X-ray magnetic circular dichroism analyses. *J Am Chem Soc* **126**(1):88–95.

Furdui, C. and Ragsdale, S.W. 2002. The roles of coenzyme A in the pyruvate: ferredoxin oxidoreductase reaction mechanism: rate enhancement of electron transfer from a radical intermediate to an iron-sulfur cluster. *Biochemistry* **41**(31):9921–9937.

Gencic, S. and Grahame, D.A. 2003. Nickel in subunit beta of the acetyl-CoA decarbonylase/synthase multienzyme complex in methanogens: Catalytic properties and evidence for a binuclear Ni-Ni site. *J Biol Chem* **278**(8):6101–6110.

Gencic, S., LeClerc, G.M., Gorlatova, N., Peariso, K., Penner-Hahn, J.E., and Grahame, D.A. 2001. Zinc-thiolate intermediate in catalysis of methyl group transfer in Methanosarcina barkeri. *Biochemistry* **40**(43):13068–13078.

Gnida, M., Ferner, R., Gremer, L., Meyer, O., and Meyer-Klaucke, W. 2003. A novel binuclear [CuSMo] cluster at the active site of carbon monoxide dehydrogenase: characterization by X-ray absorption spectroscopy. *Biochemistry* **42**(1):222–230.

Grahame, D.A. 2003. Acetate C—C bond formation and decomposition in the anaerobic world: the structure of a central enzyme and its key active-site metal cluster. *Trends Biochem Sci* **28**(5):221–224.

Grahame, D.A. and Demoll, E. 1995. Substrate and accessory protein requirements and thermodynamics of acetyl-CoA synthesis and cleavage in *Methanosarcina barkeri*. *Biochemistry* **34**(14):4617–4624.

Gu, W., Gencic, S., Cramer, S.P., and Grahame, D.A. 2003. The A-cluster in subunit beta of the acetyl-CoA decarbonylase/synthase complex from Methanosarcina thermophila: Ni and Fe K-edge XANES and EXAFS analyses. *J Am Chem Soc* **125**(50):15343–15351.

Gu, W., Seravalli, J., Ragsdale, S.W., and Cramer, S.P. 2004. CO-induced structural rearrangement of the C-cluster in *Carboxydothermus hydrogenoformans* CO dehydrogenase—evidence from Ni K-edge X-ray absorption spectroscopy. *Biochemistry* in press.

Happe, R.P., Roseboom, W., Pierik, A.J., Albracht, S.P., and Bagley, K.A. 1997. Biological activation of hydrogen. *Nature* **385**(6612):126.

Harder, S.A., Lu, W.-P., Feinberg, B.F., and Ragsdale, S.W. 1989. Spectroelectrochemical studies of the corrinoid/iron-sulfur protein from *Clostridium thermoaceticum*. *Biochemistry* **28:**9080–9087.

Hausinger, R.P. 2003. Ni and CO: more surprises. *Nat Struct Biol* **10**(4):234–236.

Heo, J., Halbleib, C.M., and Ludden, P.W. 2001a. Redox-dependent activation of CO dehydrogenase from Rhodospirillum rubrum. *Proc Natl Acad Sci USA* **98**(14):7690–7693.

Heo, J., Staples, C.R., and Ludden, P.W. 2001b. Redox-dependent CO2 reduction activity of CO dehydrogenase from Rhodospirillum rubrum. *Biochemistry* **40**(25):7604–7611.

Hino, S. and Tauchi, H. 1987. Production of carbon monoxide from aromatic amino acids by *Morganella morganii*. *Arch Microbiol* **148:**167–171.

Horner, D.S., Hirt, R.P., and Embley, T.M. 1999. A single eubacterial origin of eukaryotic pyruvate: ferredoxin oxidoreductase genes: implications for the evolution of anaerobic eukaryotes. *Mol Biol Evol* **16**(9):1280–1291.

Hsu, T., Daniel, S.L., Lux, M.F., and Drake, H.L. 1990a. Biotransformations of carboxylated aromatic compounds by the acetogen Clostridium thermoaceticum: generation of growth-supportive CO2 equivalents under CO2-limited conditions. *J Bacteriol* **172**(1):212–217.

Hsu, T., Lux, M.F., and Drake, H.L. 1990b. Expression of an aromatic-dependent decarboxylase which provides growth-essential CO_2 equivalents for the acetogenic (Wood) pathway of *Clostridium thermoaceticum*. *J Bacteriol* **172:**5901–5907.

Hu, S.-I., Drake, H.L., and Wood, H.G. 1982. Synthesis of acetyl coenzyme A from carbon monoxide, methyltetrahydrofolate, and coenzyme A by enzymes from *Clostridium thermoaceticum*. *J Bacteriol* **149**(2):440–448.

Hu, S.-I., Pezacka, E., and Wood, H.G. 1984. Acetate synthesis from carbon monoxide by *Clostridium thermoaceticum*. Purification of the corrinoid protein. *J Biol Chem* **259**(14):8892–8897.

Hu, Z.G., Spangler, N.J., Anderson, M.E., Xia, J.Q., Ludden, P.W., Lindahl, P.A., and Münck, E. 1996. Nature of the C-cluster in Ni-containing carbon monoxide dehydrogenases. *J Am Chem Soc* **118**(4):830–845.

Huber, C. and Wachtershauser, G. 1997. Activated acetic acid by carbon fixation on (Fe,Ni)S under primordial conditions [see comments]. *Science* **276**(5310):245–247.

Hugendieck, I. and Meyer, O. 1992. The structural genes encoding CO dehydrogenase subunits (cox L, M. and S) in *Pseudomonas carboxydovorans* OM5 reside on plasmid pHCG3 and are, with the exception of *Streptomyces thermoautotrophicus*, conserved in carboxydotrophic bacteria. *Arch Microbiol* **157:**301–304.

Hugenholtz, J. and Ljungdahl, L.G. 1989. Electron transport and electrochemical proton gradient in membrane vesicles of Clostridium thermoautotrophicum. *J Bacteriol* **171**(5):2873–2875.

Hughes, N.J., Chalk, P.A., Clayton, C.L., and Kelly, D.J. 1995. Identification of carboxylation enzymes and characterization of a novel four-subunit pyruvate: flavodoxin oxidoreductase from Helicobacter pylori. *J Bacteriol* **177**(14):3953–3959.

Jeon, W.B., Cheng, J., and Ludden, P.W. 2001. Purification and characterization of membrane-associated CooC protein and its functional role in the insertion of nickel into carbon monoxide dehydrogenase from Rhodospirillum rubrum. *J Biol Chem* **276**(42):38602–38609.

Johnson, J.L., Rajagopalan, K.V., and Meyer, O. 1990. Isolation and characterization of a second molybdopterin dinucleotide: molybdopterin cytosine dinucleotide. *Arch Biochem Biophys* **283:**542–545.

Kaserer, H. 1906. Die oxydation des wasserstoffes durch microorganismen. *Zentralblatt fur Bakteriologie, II Abteilung* **16:**681–696.

Kerby, R. and Zeikus, J.G. 1983. Growth of *Clostridium thermoaceticum* on H_2/CO_2 or CO as energy source. *Curr Microbiol* **8:**27–30.

Kerby, R.L., Ludden, P.W., and Roberts, G.P. 1997. In vivo nickel insertion into the carbon monoxide dehydrogenase of Rhodospirillum rubrum: molecular and physiological characterization of cooCTJ. *J Bacteriol* **179**(7):2259–2266.

Kerscher, L. and Oesterhelt, D. 1982. Pyruvate: ferredoxin oxidoreductase—new findings on an ancient enzyme. *Trends Biochem Sci* **7**(October):371–374.

Kletzin, A. and Adams, M.W.W. 1996. Molecular and phylogenetic characterization of pyruvate and 2-ketoisovalerate ferredoxin oxidoreductases from *Pyrococcus furiosus* and pyruvate ferredoxin oxidoreductase from *Thermotoga maritima*. *J Bacteriol* **178**(1):248–257.

Kumar, M., Lu, W.-P., Liu, L., and Ragsdale, S.W. 1993. Kinetic evidence that CO dehydrogenase catalyzes the oxidation of CO and the synthesis of acetyl-CoA at separate metal centers. *J Am Chem Soc* **115:**11646–11647.

Kumar, M., Lu, W.-P., and Ragsdale, S.W. 1994. Binding of carbon disufide to the site of acetyl-CoA synthesis by the nickel-iron-sulfur protein, CO dehydrogenase, from *Clostridium thermoaceticum*. *Biochemistry* **33:**9769–9777.

Kumar, M. and Ragsdale, S.W. 1992. Characterization of the CO binding site of carbon monoxide dehydrogenase from *Clostridium thermoaceticum* by infrared spectroscopy. *J Am Chem Soc* **114:**8713–8715.

Lantzsch, K. 1922. Actinomyces oligocarbophyilus (Bacillus oligocarbophilus Beij.), sein formwechsel und seine physiologie. *Zentralblat fur Bakteriologie, II Abteilung* **57:**309–319.

Lanzilotta, W.N., Schuller, D.J., Thorsteinsson, M.V., Kerby, R.L., Roberts, G.P., and Poulos, T.L. 2000. Structure of the CO sensing transcription activator CooA. *Nat Struct Biol* **7:**876–880.

Lebertz, H., Simon, H., Courtney, L.F., Benkovic, S.J., Zydowsky, L.D., Lee, K., and Floss, H.G. 1987. Stereochemistry of acetic acid formation from 5-methyl-tetrahydrofolate by *Clostridium thermoaceticum*. *J Am Chem Soc* **109:**3173–3174.

Leduc, J., Thorsteinsson, M.V., Gaal, T., and Roberts, G.P. 2001. Mapping CooA.RNA polymerase interactions. Identification of activating regions 2 and 3 in CooA, the co-sensing transcriptional activator. *J Biol Chem* **276**(43):39968–39973.

Lin, W. and Whitman, W.B. 2004. The importance of porE and porF in the anabolic pyruvate oxidoreductase of Methanococcus maripaludis. *Arch Microbiol* **181:**68–73.

Lin, W.C., Yang, Y.L., and Whitman, W.B. 2003. The anabolic pyruvate oxidoreductase from Methanococcus maripaludis. *Arch Microbiol* **179**(6):444–456.

Linck, R.C., Spahn, C.W., Rauchfuss, T.B., and Wilson, S.R. 2003. Structural analogues of the bimetallic reaction center in acetyl CoA synthase: a Ni—Ni model with bound CO. *J Am Chem Soc* **125**(29):8700–8701.

Lindahl, P.A. 2002. The Ni-containing carbon monoxide dehydrogenase family: light at the end of the tunnel? *Biochemistry* **41**(7):2097–2105.

Lindahl, P.A. 2004. Acetyl-coenzyme A synthase: The case for a Ni_p^0-based mechanism of catalysis. *J Biol Inorg Chem*, in press.

Lindahl, P.A., Münck, E., and Ragsdale, S.W. 1990a. CO dehydrogenase from *Clostridium thermoaceticum*: EPR and electrochemical studies in CO_2 and argon atmospheres. *J Biol Chem* **265:**3873–3879.

Lindahl, P.A., Ragsdale, S.W., and Münck, E. 1990b. Mössbauer studies of CO dehydrogenase from *Clostridium thermoaceticum*. *J Biol Chem* **265:**3880–3888.

Ljungdahl, L.G. 1986. The autotrophic pathway of acetate synthesis in acetogenic bacteria. *Ann Rev Microbiol* **40:**415–450.

Ljungdahl, L.G. and Andreesen, J.R. 1978. Formate dehydrogenase, a selenium-tungsten enzyme from *Clostridium thermoaceticum*. *Methods Enzymol* **53:**360–372.

Ljungdahl, L.G., O'Brien, W.E., Moore, M.R., and Liu, M.T. 1980. Methylenetetrahydrofolate dehydrogenase from *Clostridium* formicoaceticum and methylenetetrahydrofolate dehydrogenase, methenyltetrahydrofolate cyclohydrolase (combined) from *Clostridium thermoaceticum*. *Methods Enzymol* **66:**599–609.

Loke, H.K. and Lindahl, P.A. 2003. Identification and preliminary characterization of AcsF, a putative Ni-insertase used in the biosynthesis of acetyl-CoA synthase from Clostridium thermoaceticum. *J Inorg Biochem* **93**(1–2):33–40.

Lovell, C.R., Przybyla, A., and Ljungdahl, L.G. 1990. Primary structure of the thermostable formyltetrahydrofolate synthetase from *Clostridium thermoaceticum*. *Biochemistry* **29:**5687–5694.

Lukehart, C.M. 1985. *Fundamental transition metal organometallic chemistry*, Brooks/Cole, Monterey, CA.

Martin, B.D. and Finke, R.G. 1990. Co-C homolysis and bond dissociation energy studies of biological alkylcobalamins: methylcobalamin, including a $\geq 10^{15}$ Co-CH_3 homolysis rate enhancement at 25°C following one-electron reduction. *J Am Chem Soc* **112:**2419–2420.

Matthews, R.G. 2001. Cobalamin-dependent methyltransferases. *Acc Chem Res* **34**(8):681–689.

Matthews, R.G. and Goulding, C.W. 1997. Enzyme-catalyzed methyl transfers to thiols: the role of zinc. *Curr Opin Chem Biol* **1**(3):332–339.

Maynard, E.L. and Lindahl, P.A. 1999. Evidence of a molecular tunnel connecting the active sites for CO_2 reduction and acetyl-CoA synthesis in acetyl-CoA synthase from *Clostridium thermoaceticum*. *J Am Chem Soc* **121:**9221–9222.

Maynard, E.L. and Lindahl, P.A. 2001. Catalytic coupling of the active sites in acetyl-CoA synthase, a bifunctional CO-channeling enzyme. *Biochemistry* **40**(44):13262–13267.

Maynard, E.L., Sewell, C., and Lindahl, P.A. 2001. Kinetic mechanism of acetyl-CoA synthase: steady-state synthesis at variable CO/CO_2 pressures. *J Am Chem Soc* **123**(20):4697–4703.

Menendez, C., Bauer, Z., Huber, H., Gad'on, N., Stetter, K.O., and Fuchs, G. 1999. Presence of acetyl coenzyme A (CoA) carboxylase and propionyl-CoA carboxylase in autotrophic Crenarchaeota and indication for operation of a 3-hydroxypropionate cycle in autotrophic carbon fixation. *J Bacteriol* **181**(4):1088–1098.

Menon, S. and Ragsdale, S.W. 1996a. Evidence that carbon monoxide is an obligatory intermediate in anaerobic acetyl-CoA synthesis. *Biochemistry* **35**(37):12119–12125.

Menon, S. and Ragsdale, S.W. 1996b. Unleashing hydrogenase activity in pyruvate: ferredoxin oxidoreductase and acetyl-CoA synthase/CO dehydrogenase. *Biochemistry* **35**(49):15814–15821.

Menon, S. and Ragsdale, S.W. 1997. Mechanism of the *Clostridium thermoaceticum* pyruvate: ferredoxin oxidoreductase: evidence for the common catalytic intermediacy of the hydroxyethylthiamine pyropyrosphate radical. *Biochemistry* **36:**8484–8494.

Menon, S. and Ragsdale, S.W. 1998. Role of the [4Fe-4S] cluster in reductive activation of the cobalt center of the corrinoid iron-sulfur protein from *Clostridium thermoaceticum* during acetyl-CoA synthesis. *Biochemistry* **37**(16):5689–5698.

Menon, S. and Ragsdale, S.W. 1999. The role of an iron-sulfur cluster in an enzymatic methylation reaction: methylation of CO dehydrogenase/acetyl-CoA synthase by the methylated corrinoid iron-sulfur protein. *J Biol Chem* **274**(17):11513–11518.

Meuer, J., Kuettner, H.C., Zhang, J.K., Hedderich, R., and Metcalf, W.W. 2002. Genetic analysis of the archaeon *Methanosarcina barkeri* Fusaro reveals a central role for Ech hydrogenase and ferredoxin in methanogenesis and carbon fixation. *Proc Natl Acad Sci USA* **99**(8):5632–5637.

Meyer, O., Frunzke, K., Gadkari, D., Jacobitz, S., Hugendieck, I., and Kraut, M. 1990. Utilization of carbon monoxide by aerobes: recent advances. *FEMS Microbiol Rev* **87:**253–260.

Meyer, O., Frunzke, K., and Mörsdorf, G. 1993. Biochemistry of the aerobic utilization of carbon monoxide. In *Microbial growth on C_1 compounds*, pp. 433–459. J.C. Murrell, and D.P. Kelly, Eds., Intercept, Ltd., Andover, MA.

Meyer, O., Jacobitz, S., and Kruger, B. 1986. Biochemistry and physiology of aerobic carbon monoxide-utilizing bacteria. *FEMS Microbiol Rev* **39:**161–179.

Meyer, O. and Rhode, M. 1984. Enzymology and bioenergetics of carbon monoxide-oxidizing bacteria. In *Microbial growth on C1 compounds*, pp. 26–33. R.L. Crawford, and R.S. Hanson, Eds., American Society for Microbiology, Washington, DC.

Meyer, O. and Schlegel, H.G. 1983. Biology of aerobic carbon monoxide-oxidizing bacteria. *Ann Rev Microbiol* **37:**277–310.

Montet, Y., Amara, P., Volbeda, A., Vernede, X., Hatchikian, E.C., Field, M.J., Frey, M., and Fontecilla-Camps, J.C. 1997. Gas access to the active site of Ni-Fe hydrogenases probed by X-ray crystallography and molecular dynamics [letter]. *Nat Struct Biol* **4**(7):523–526.

Moore, M.R., O'Brien, W.E., and Ljungdahl, L.G. 1974. Purification and characterization of nicotinamide adenine dinucleotide-dependent methylenetetrahydrofolate dehydrogenase from *Clostridium formicoaceticum*. *J Biol Chem* **249:**5250–5253.

Morita, T., Perrella, M.A., Lee, M.E., and Kourembanas, S. 1995. Smooth muscle cell-derived carbon monoxide is a regulator of vascular cGMP. *Proc Natl Acad Sci USA* **92**(5):1475–1479.

Nicolet, Y., Lemon, B.J., Fontecilla-Camps, J.C. and Peters, J.W. 2000. A novel FeS cluster in Fe-only hydrogenases. *Trends Biochem Sci* **25**(3):138–143.

O'Brien, W.E., Brewer, J.M., and Ljungdahl, L.G. 1973. Purification and characterization of thermostable 5,10- methylenetetrahydrofolate dehydrogenase from *Clostridium thermoaceticum*. *J Biol Chem* **248:**403–408.

Otting, G., Liepinsh, E., Halle, B., and Frey, U. 1997. NMR identification of hydrophobic cavities with low water occupancies in protein structures using small gas molecules. *Nat Struct Biol* **4**(5):396–404.

Page, C.C., Moser, C.C., Chen, X.X., and Dutton, P.L. 1999. Natural engineering principles of electron tunnelling in biological oxidation-reduction. *Nature* **402**(6757):47–52.

Park, E.Y., Clark, J.E., DerVartanian, D.V., and Ljungdahl, L.G. 1991. 5,10-methylenetetrahydrofolate reductases: iron-sulfur-zinc flavoproteins of two acetogenic clostridia. In *Chemistry Biochemstry Flavoenzymes*, Vol. 1, pp. 389–400. F. Miller, Ed., CRC Press, Boca Raton, FL.

Pearson, D.M., Oreilly, C., Colby, J., and Black, G.W. 1994. DNA sequence of the cut A, B and C genes, encoding the molybdenum containing hydroxylase carbon monoxide dehydrogenase, from Pseudomonas thermocarboxydovorans strain C2. *Bba-Bioenergetics* **1188**(3):432–438.

Peters, J.W., Lanzilotta, W.N., Lemon, B.J., and Seefeldt, L.C. 1998. X-ray crystal structure of the Fe-only hydrogenase (Cpl) from Clostridium pasteurianum to 1.8 angstrom resolution. *Science* **282**(5395):1853–1858.

Pezacka, E. and Wood, H.G. 1984. Role of carbon monoxide dehydrogenase in the autotrophic pathway used by acetogenic bacteria. *Proc Natl Acad Sci USA* **81:**6261–6265.

Pieulle, L., Charon, M.H., Bianco, P., Bonicel, J., Petillot, Y., and Hatchikian, E.C. 1999. Structural and kinetic studies of the pyruvate-ferredoxin oxidoreductase/ferredoxin complex from Desulfovibrio africanus. *Eur J Biochem* **264**(2):500–508.

Ragsdale, S.W. 1991. Enzymology of the acetyl-CoA pathway of CO_2 fixation. *CRC Crit Rev Biochem Mol Biol* **26:**261–300.

Ragsdale, S.W. 2003a. Anaerobic one-carbon catalysis. In *Encyclopedia of catalysis*, Vol. 1, pp. 665–695. I.T. Horvath, E. Iglesia, M.T. Klein, J.A. Lercher, A.J. Russell, and E.I. Stiefel, Eds., John Wiley and Sons, Inc., New York.

Ragsdale, S.W. 2003b. Pyruvate: ferredoxin oxidoreductase and its radical intermediate. *Chemical Reviews* **103**(6):2333–2346.

Ragsdale, S.W., Clark, J.E., Ljungdahl, L.G., Lundie, L.L., and Drake, H.L. 1983a. Properties of purified carbon monoxide dehydrogenase from *Clostridium thermoaceticum* a nickel, iron-sulfur protein. *J Biol Chem* **258:**2364–2369.

Ragsdale, S.W. and Kumar, M. 1996. Ni containing carbon monoxide dehydrogenase/acetyl-CoA synthase. *Chem Rev* **96**(Nov, No. 7):2515–2539.

Ragsdale, S.W., Lindahl, P.A., and Münck, E. 1987. Mössbauer, EPR, and optical studies of the corrinoid/Fe-S protein involved in the synthesis of acetyl-CoA by *Clostridium thermoaceticum*. *J Biol Chem* **262:**14289–14297.

Ragsdale, S.W. and Ljungdahl, L.G. 1984a. Hydrogenase from *Acetobacterium woodii*. *Arch Microbiol* **139:**361–365.

Ragsdale, S.W. and Ljungdahl, L.G. 1984b. Purification and properties of NAD-dependent 5,10-methylenetetrahydrofolate dehydrogenase from Acetobacterium woodii. *J Biol Chem* **259:**3499–3503.

Ragsdale, S.W., Ljungdahl, L.G., and DerVartanian, D.V. 1983b. ^{13}C and ^{61}Ni isotope substitution confirm the presence of a nickel(III)-carbon species in acetogenic CO dehydrogenases. *Biochem Biophys Res Commun* **115**(2):658–665.

Ragsdale, S.W. and Wood, H.G. 1985. Acetate biosynthesis by acetogenic bacteria: evidence that carbon monoxide dehydrogenase is the condensing enzyme that catalyzes the final steps of the synthesis. *J Biol Chem* **260:**3970–3977.

Ragsdale, S.W., Wood, H.G., and Antholine, W.E. 1985. Evidence that an iron-nickel-carbon complex is formed by reaction of CO with the CO dehydrogenase from *Clostridium thermoaceticum*. *Proc Natl Acad Sci USA* **82:**6811–6814.

Ram, M.S. and Riordan, C.G. 1995. Methyl transfer from a cobalt complex to Ni(tmc)(+) yielding Ni(tmc)Me(+): a model for methylcobalamin alkylation of CO dehydrogenase. *J Am Chem Soc* **117**(8):2365–2366.

Ram, M.S., Riordan, C.G., Yap, G.P.A., Liable-Sands, L., Rheingold, A.L., Marchaj, A., and Norton, J.R. 1997. Kinetics and mechanism of alkyl transfer from organocobalt(III) to nickel(I): implications for the synthesis of acetyl coenzyme A by CO dehydrogenase. *J Am Chem Soc* **119**(7):1648–1655.

Rees, D.C. 2002. Great metalloclusters in enzymology. *Annu Rev Biochem* **71:**221–246.

Roberts, D.L., James-Hagstrom, J.E., Smith, D.K., Gorst, C.M., Runquist, J.A., Baur, J.R., Haase, F.C., and Ragsdale, S.W. 1989. Cloning and expression of the gene cluster encoding key proteins involved in acetyl-CoA synthesis in *Clostridium thermoaceticum*: CO dehydrogenase, the corrinoid/Fe-S protein, and methyltransferase. *Proc Natl Acad Sci USA* **86:**32–36.

Roberts, D.L., Zhao, S., Doukov, T., and Ragsdale, S.W. 1994. The reductive acetyl-CoA pathway: sequence and heterologous expression of active CH_3-H_4 folate: corrinoid/iron sulfur protein methyltransferase from *Clostridium themoaceticum*. *J Bacteriol* **176:**6127–6130.

Russell, M.J., Daia, D.E., and Hall, A.J. 1998b. The emergence of life from FeS bubbles at alkaline hot springs in an acid ocean. In *Thermophiles: the keys to molecular evolution and the origin of life?* pp. 77–126. M.W.W. Adams, L.G. Ljungdahl, and J. Wiegel, Eds., Taylor and Francis, Washington, DC.

Russell, M.J. and Hall, A.J. 1997. The emergence of life from iron monosulphide bubbles at a submarine hydrothermal redox and pH front. *J Geol Soc London* **154:**337–402.

Russell, W.K., Stalhandske, C.M.V., Xia, J.Q., Scott, R.A., and Lindahl, P.A. 1998. Spectroscopic, redox, and structural characterization of the Ni-labile and nonlabile forms of the acetyl-CoA synthase active. Site of carbon monoxide dehydrogenase. *J Am Chem Soc* **120**(30):7502–7510.

Santiago, B. and Meyer, O. 1996. Characterization of hydrogenase activities associated with the molybdenum CO dehydrogenase from *Oligotropha carboxidovorans*. *FEMS Microbiol Lett* **136**(2):157–162.

Schenker, R.P. and Brunold, T.C. 2003. Computational studies on the A cluster of acetyl-coenzyme A synthase: geometric and electronic properties of the NiFeC species and mechanistic implications. *J Am Chem Soc* **125**(46):13962–13963.

Schidlowski, M., Hayes, J.M., and Kaplan, I.R. 1983. In *Earth's earliest biosphere: its origin and evolution*, pp. 149–186. J.W. Schopf, Ed., Princeton Univ. Press, Princeton, NJ.

Schiltz, M., Fourme, R., and Prange, T. 2003. Use of noble gases xenon and krypton as heavy atoms in protein structure determination. *Methods Enzymol* **374:**83–119.

Schubel, U., Kraut, M., Mörsdorf, G., and Meyer, O. 1995. Molecular characterization of the gene cluster coxMSL encoding the molybdenum-containing carbon monoxide dehydrogenase of *Oligotropha carboxidovorans*. *J Bacteriol* **177**(8):2197–2203.

Seravalli, J., Gu, W., Tam, A., Strauss, E., Begley, T.P., Cramer, S.P., and Ragsdale, S.W. 2003. Functional copper at the acetyl-CoA synthase active site. *Proc Natl Acad Sci USA* **100:**3689–3694.

Seravalli, J., Kumar, M., Lu, W.-P., and Ragsdale, S.W. 1997. Mechanism of carbon monoxide oxidation by the carbon monoxide dehydrogenase/acetyl-CoA synthase from *Clostridium thermoaceticum*: kinetic characterization of the intermediates. *Biochemistry* **36:**11241–11251.

Seravalli, J., Kumar, M., and Ragsdale, S.W. 2002. Rapid kinetic studies of acetyl-CoA synthesis: evidence supporting the catalytic intermediacy of a paramagnetic NiFeC species in the autotrophic Wood-Ljungdahl pathway. *Biochemistry* **41**(6):1807–1819.

Seravalli, J. and Ragsdale, S.W. 2000. Channeling of carbon monoxide during anaerobic carbon dioxide fixation. *Biochemistry* **39**(6):1274–1277.

Seravalli, J., Xiao, Y., Gu, W., Cramer, S.P., Antholine, W.E., Krymov, V., Gerfen, G.J., and Ragsdale, S.W. 2004. Evidence that Ni-Ni acetyl-CoA synthase is active and that the Cu-Ni enzyme is not. *Biochemistry* **43**(13):3944–3955.

Seravalli, J., Zhao, S., and Ragsdale, S.W. 1999. Mechanism of transfer of the methyl group from (6S)-methyltetrahydrofolate to the corrinoid/iron-sulfur protein catalyzed by the methyltransferase from Clostridium thermoaceticum: a key step in the Wood-Ljungdahl pathway of acetyl-CoA synthesis. *Biochemistry* **38**(18):5728–5735.

Shanmugasundaram, T., Kumar, G.K., and Wood, H.G. 1988. Involvement of tryptophan residues at the coenzyme A binding site of carbon monoxide dehydrogenase from *Clostridium thermoaceticum*. *Biochemistry* **27:**6499–6503.

Shanmugasundaram, T., Sundaresh, C.S., and Kumar, G.K. 1993. Identification of a cysteine involved in the interaction between carbon monoxide dehydrogenase and corrinoid/Fe-S protein from *Clostridium thermoaceticum*. *FEBS Lett* **326**(July):281–284.

Shanmugasundaram, T. and Wood, H.G. 1992. Interaction of ferredoxin with carbon monoxide dehydrogenase from *Clostridium thermoaceticum*. *J Biol Chem* **267**(Jan. 15):897–900.

Shelver, D., Kerby, R.L., He, Y.P., and Roberts, G.P. 1995. Carbon monoxide-induced activation of gene expression in *Rhodospirillum rubrum* requires the product of cooA, a member of the cyclic AMP receptor protein family of transcriptional regulators. *J Bacteriol* **177**(8):2157–2163.

Shelver, D., Kerby, R.L., He, Y.P., and Roberts, G.P. 1997. CooA, a CO-sensing transcription factor from Rhodospirillum rubrum, is a CO-binding heme protein. *Proc Natl Acad Sci USA* **94**(21):11216–11220.

Shin, W., Anderson, M.E., and Lindahl, P.A. 1993. Heterogeneous nickel environments in carbon monoxide dehydrogenase from *Clostridium thermoaceticum*. *J Am Chem Soc* **115:**5522–5526.

Shin, W. and Lindahl, P.A. 1992. Function and CO binding properties of the NiFe complex in carbon monoxide dehydrogenase from *Clostridium thermoaceticum*. *Biochemistry* **31:**12870–12875.

Song, H.K., Mulrooney, S.B., Huber, R., and Hausinger, R.P. 2001. Crystal structure of Klebsiella aerogenes UreE, a nickel-binding metallochaperone for urease activation. *J Biol Chem* **276**(52):49359–49364.

Soupene, E., Chu, T., Corbin, R.W., Hunt, D.F., and Kustu, S. 2002a. Gas channels for NH(3): proteins from hyperthermophiles complement an Escherichia coli mutant. *J Bacteriol* **184**(12):3396–3400.

Soupene, E., King, N., Feild, E., Liu, P., Niyogi, K.K., Huang, C.H., and Kustu, S. 2002b. Rhesus expression in a green alga is regulated by CO(2). *Proc Natl Acad Sci USA* **99**(11):7769–7773.

Sun, A.Y., Ljungdahl, L., and Wood, H.G. 1969. Total synthesis of acetate from CO_2. II. Purification and properties of formyltetrahydrofolate synthetase from *Clostridium thermoaceticum*. *J Bacteriol* **98**(2):842–844.

Svetlichny, V.A., Sokolova, T.G., Gerhardt, M., Ringpfeil, M., Kostrikina, N.A., and Zavarzin, G.A. 1991. Carboxydothermus hydrogenoformans gen. nov., sp. nov., a CO-utilizing thermophilic anaerobic bacterium from hydrothermal environments of Kunashir island. *Syst Appl Microbiol* **14:**254–260.

Svetlitchnyi, V., Dobbek, H., Meyer-Klaucke, W., Meins, T., Thiele, B., Romer, P., Huber, R., and Meyer, O. 2004. A functional Ni-Ni-[4Fe-4S] cluster in the monomeric acetyl-CoA synthase from Carboxydothermus hydrogenoformans. *Proc Natl Acad Sci USA* **101**(2):446–451.

Svetlitchnyi, V., Peschel, C., Acker, G., and Meyer, O. 2001. Two membrane-associated NiFeS-carbon monoxide dehydrogenases from the anaerobic carbon-monoxide-utilizing eubacterium Carboxydothermus hydrogenoformans. *J Bacteriol* **183**(17):5134–5144.

Tan, G.O., Ensign, S.A., Ciurli, S., Scott, M.J., Hedman, B., Holm, R.H., Ludden, P.W., Korszun, Z.R., Stephens, P.J., and Hodgson, K.O. 1992. On the structure of the nickel/iron/sulfur center of the carbon monoxide dehydrogenase from *Rhodospirillum rubrum*: An x-ray absorption spectroscopy study. *Proc Natl Acad Sci USA* **89:**4427–4431.

Tan, X., Sewell, C., Yang, Q., and Lindahl, P.A. 2003. Reduction and methyl transfer kinetics of the alpha subunit from acetyl coenzyme A synthase. *J Am Chem Soc* **125**(2):318–319.

Tan, X.S., Sewell, C., and Lindahl, P.A. 2002. Stopped-flow kinetics of methyl group transfer between the corrinoid-iron-sulfur protein and acetyl-coenzyme A synthase from Clostridium thermoaceticum. *J Am Chem Soc* **124**(22):6277–6284.

Tenhunen, R., Marver, H.S., and Schmid, R. 1969. Microsomal heme oxygenase. Characterization of the enzyme. *J Biol Chem* **244**(23):6388–6394.

Tersteegen, A., Linder, D., Thauer, R.K., and Hedderich, R. 1997. Structures and functions of four anabolic 2-oxoacid oxidoreductases in Methanobacterium thermoautotrophicum. *Eur J Biochem* **244**(3):862–868.

Thauer, R.K. 1998. Biochemistry of methanogenesis: a tribute to Marjory Stephenson. *Microbiol UK* **144:**2377–2406.

Uffen, R.L. 1983. Metabolism of carbon monoxide by *Rhodopseudomonas gelatinosa*: cell growth and properties of the oxidative system. *J Bacteriol* **155:**956–965.

Uyeda, K. and Rabinowitz, J.C. 1971. Pyruvate-ferredoxin oxidoreductase. 3. Purification and properties of the enzyme. *J Biol Chem* **246**(10):3111–3119.

Verma, A., Hirsch, D.J., Glatt, C.E., Ronnett, G.V., and Snyder, S.H. 1993. Carbon monoxide: a putative neural messenger. *Science* **259:**381–384.

Vobeda, A. and Fontecilla-Camps, J.C. 2004. Crystallographic evidence for a CO/CO2 tunnel gating mechanism in the bifunctional carbon monoxide dehydrogenase/ acetyl Coenzyme A synthase from *Moorella thermoacetica*. *J Biol Inorg Chem* in press.

Wahl, R.C. and Orme-Johnson, W.H. 1987. Clostridial pyruvate oxidoreductase and the pyruvate oxidizing enzyme specific to nitrogen fixation in *Klebsiella pneumoniae* are similar enzymes. *J Biol Chem* **262:**10489–10496.

Warthen, C.R., Hammes, B.S., Carrano, C.J., and Crans, D.C. 2001. Methylation of neutral pseudotetrahedral zinc thiolate complexes: model reactions for alkyl group transfer to sulfur by zinc-containing enzymes. *J Biol Inorg Chem* **6**(1):82–90.

Watt, R.K. and Ludden, P.W. 1998. The identification, purification, and characterization of CooJ. A nickel-binding protein that is co-regulated with the Ni-containing CO dehydrogenase from Rhodospirillum rubrum. *J Biol Chem* **273**(16):10019–10025.

Watt, R.K. and Ludden, P.W. 1999. Nickel-binding proteins. *Cell Mol Life Sci* **56**(7–8):604–625.

Webster, C.E., Darensbourg, M.Y., Lindahl, P.A., and Hall, M.B. 2004. Structures and energetics of models for the active site of acetylcoenzyme a synthase: role of distal and proximal metals in catalysis. *J Am Chem Soc* **126**(11):3410–3411.

Wirt, M.D., Kumar, M., Ragsdale, S.W., and Chance, M.R. 1993. X-ray absorption spectroscopy of the corrinoid/iron sulfur protein involved in acetyl-CoA synthesis by *Clostridium thermoaceticum*. *J Am Chem Soc* **115:**2146–2150.

Wirt, M.D., Wu, J.-J., Scheuring, E.M., Kumar, M., Ragsdale, S.W., and Chance, M.R. 1995. Structural and electronic factors in heterolytic cleavage: formation of the Co(I) intermediate in the corrinoid/iron-sulfur protein from *Clostridium thermoaceticum*. *Biochemistry* **34**(15):5269–5273.

Wolin, M.J. and Miller, T.L. 1994. Acetogenesis from CO_2 in the human colonic ecosystem. In *Acetogenesis*, pp. 365–385. H.L. Drake, Ed., Chapman and Hall, New York.

Xia, J., Sinclair, J.F., Baldwin, T.O., and Lindahl, P.A. 1996. Carbon monoxide dehydrogenase from Clostridium thermoaceticum: quaternary structure, stoichiometry of its SDS-induced dissociation, and characterization of the faster-migrating form. *Biochemistry* **35**(6):1965–1971.

Yagi, T. 1959. Enzymic oxidation of carbon monoxide. *Biochim Biophys Acta* **30:**194–195.

Yamamoto, K., Ishikawa, H., Takahashi, S., Ishimori, K., Morishima, I., Nakajima, H., and Aono, S. 2001. Binding of CO at the Pro2 side is crucial for the activation of CO-sensing transcriptional activator CooA. 1H NMR spectroscopic studies. *J Biol Chem* **276:**11473–11476.

Youn, H., Kerby, R.L., Conrad, M., and Roberts, G.P. 2004. Functionally critical elements of CooA-related CO sensors. *J Bacteriol* **186**(5):1320–1329.

Zhao, S., Roberts, D.L., and Ragsdale, S.W. 1995. Mechanistic studies of the methyltransferase from *Clostridium thermoaceticum*: origin of the pH dependence of the methyl group transfer from methyltetrahydrofolate to the corrinoid/iron-sulfur protein. *Biochemistry* **34:**15075–15083.

Zhao, S.Y. and Ragsdale, S.W. 1996. A conformational change in the methyltransferase from *Clostridium thermoaceticum* facilitates the methyl transfer from (6S)-methyltetrahydrofolate to the corrinoid iron- sulfur protein in the sacetyl-CoA pathway. *Biochemistry* **35**(7):2476–2481.